



A Dynamic Network Model of the Unsecured Interbank Lending Market

Francisco Blasques, Falk Bräuning, and Iman van Lelyveld

Abstract:

We introduce a dynamic network model of interbank lending and estimate the parameters by indirect inference using network statistics of the Dutch interbank market from mid-February 2008 through April 2011. We find that credit-risk uncertainty and peer monitoring are significant factors in explaining the market's sparse core-periphery structure and the presence of relationship lending. Shocks to credit-risk uncertainty lead to extended periods of low market activity, intensified by a reduction in peer monitoring. Moreover, changes in the central bank's interest-rate corridor have a direct effect on the market as well as an indirect effect that acts to change banks' monitoring efforts.

JEL Classifications: C33, C51, E52, G01, G21

Keywords: interbank liquidity, financial networks, credit-risk uncertainty, peer monitoring, monetary policy, trading relationships, indirect parameter estimation

Francisco Blasques is an assistant professor of economics at VU University Amsterdam and the Tinbergen Institute. His e-mail address is f.blasques@vu.nl. Falk Bräuning, the corresponding author, is an economist in the research department at the Federal Reserve Bank of Boston. His e-mail address is falk.brauning@bos.frb.org. Iman van Lelyveld is a senior policy advisor with De Nederlandsche Bank. His e-mail address is I.P.P.van.Lelyveld@dnb.nl.

The authors thank Henrique Basso, Darrell Duffie, Lucy Gornicka, Siem Jan Koopman, Marco van der Leij, Andre Lucas, Patrick McGuire, Albert Menkveld, Joe Peek, Gabriel Perez Quiros, Gerhard Rünstler, and Hyun Song Shin for comments. Participants at seminars at De Nederlandsche Bank, Deutsche Bundesbank, the Bank of England, the Bank for International Settlements, the Duisenberg School of Finance, the ECB Money Market Workshop, the Cambridge Workshop on Financial Risk and Network Theory, the Seventh Annual SoFiE Conference, the First Annual IAAE Conference, the Banque de France-SoFiE Conference on Systemic Risk and Financial Regulation, and the GENED Workshop on Networks in Macroeconomics and Finance also provided useful feedback. We thank Elizabeth Murry for providing language and grammar suggestions and comments. Blasques and Bräuning gratefully acknowledge financial support from the Netherlands Organisation for Scientific Research and the SWIFT Institute.

This paper presents preliminary analysis and results intended to stimulate discussion and critical comment. The views expressed herein are those of the authors and do not indicate concurrence by the De Nederlandsche Bank, the Eurosystem, the Federal Reserve Bank of Boston, the principals of the Board of Governors, or the Federal Reserve System.

This paper, which may be revised, is available on the web site of the Federal Reserve Bank of Boston at <http://www.bostonfed.org/economic/wp/index.htm>.

This version: April, 2016

1 INTRODUCTION

The global financial crisis of 2007–2008 highlighted the crucial role of interbank lending markets, both in the financial system and the real economy. In particular, after Lehman Brothers collapsed in September 2008, increased uncertainty in the banking system led to severe distress in unsecured interbank lending markets. As a result, monetary policy implementation was hampered and credit supply to the nonfinancial sector declined substantially, with adverse consequences for both the financial sector and the real economy. In order to mitigate these adverse effects, central banks intervened by injecting additional liquidity into the banking sector and by adjusting their monetary policy instruments. As a consequence, central banks became the primary intermediaries for large parts of the money market during the crisis.¹

But should central banks also serve as a central counterparty for money markets during normal times? Generally, having a central counterparty for an unsecured interbank market reduces contagion effects through bilateral credit exposures (see Allen and Gale 2000). Likewise, search frictions resulting from asymmetric information about the liquidity positions of other banks are mitigated. On the other hand, with a central counterparty, private information that banks have about the credit risk posed by other banks is no longer reflected in the price at which banks can obtain funds, a situation that impairs market discipline. Moreover, the incentives for banks to acquire and process such information are largely eliminated. Indeed, as Rochet and Tirole (1996) argue, the operation of a decentralized interbank lending market must be motivated by the benefits of peer monitoring.² Consequently, in order to assess the benefits of a decentralized unsecured interbank market, one has to gauge the extent to which credit-risk uncertainty and peer monitoring affect the liquidity allocation among banks.

Our paper contributes to this debate by introducing and estimating a dynamic network model to

¹See Cœuré (2013) and Heijmans, Heuver, Levallois, and van Lelyveld (2014), video 3 for evidence of the Dutch central bank’s role.

²The European Central Bank (ECB) highlights the role of peer monitoring and private information as well: “Specifically, in the unsecured money markets, where loans are uncollateralised, interbank lenders are directly exposed to losses if the interbank loan is not repaid. This gives lenders incentives to collect information about borrowers and to monitor them over the lifetime of the interbank loan ... Therefore, unsecured money markets play a key peer monitoring role.” See the speech by Benoît Cœuré, Member of the Executive Board of the ECB, at the Morgan Stanley 16th Annual Global Investment seminar, Tourrettes, Provence, June 16, 2012. <http://www.ecb.europa.eu/press/key/date/2012/html/sp120616.en.html>, retrieved October 10, 2013.

analyze the role of peer monitoring in the unsecured interbank lending market. The key economic drivers of the model’s outcomes are asymmetric information about counterparty risk and liquidity conditions elsewhere in the market. In particular, our model focuses on the role that peer monitoring plays in reducing bank-to-bank credit-risk uncertainty and that endogenous counterparty selection (directed counterparty search) plays in mitigating search frictions resulting from the over-the-counter market structure. We estimate the network model with an indirect inference estimator (Gourieroux, Monfort, and Renault 1993) using auxiliary statistics that characterize the structure of the trading relationships and the distribution of loan conditions, as observed from transaction-level data on unsecured overnight loans made among the 50 largest Dutch banks between mid-February 2008 through April 2011.³ Using the estimated model, we then analyze how peer monitoring affects the liquidity allocation across bank pairs, how the allocation changes in response to shocks to credit-risk uncertainty, and how monetary policy can affect banks’ peer monitoring incentives.

Our estimation results show that banks’ monitoring efforts significantly reduce the bank-to-bank credit-risk uncertainty that prevails in the market. In particular, we find that peer monitoring aligned with endogenous counterparty selection generates an amplification mechanism that lies at the core of our estimated model: Lending banks invest in monitoring those borrowers whom they expect to be profitable, either because of large loan volumes, high expected returns on granted loans, or because of a high frequency of borrowing contacts. Borrowing banks obtain part of the surplus generated by peer monitoring, which strengthens their relationship with the lending bank. As a consequence of this monitoring, uncertainty about credit risk is reduced, more loans are granted, and lender banks further increase their monitoring efforts in expectation of greater profits. Thus, monitoring efforts have a multiplier effect that has important implications for the endogenous network structure as well as for the amplification of shocks to credit-risk uncertainty and changes in monetary policy.

First, we find that peer monitoring, search frictions, and uncertainty about counterparty risk assume significant roles when matching the observed trading network’s topology—notably, its high

³Specifically, our indirect inference estimator is based on an auxiliary vector that contains network statistics (for example, density, reciprocity, and centrality) that have become popular in characterizing the topological structure of interbank markets (see, for instance, Bech and Atalay 2010). We further complement these network statistics with moment statistics of bilateral interest rates and volumes, and measures of bilateral lending relationships as in Furfine (1999) and Cocco, Gomes, and Martins (2009). Our indirect inference estimator is then obtained as the parameter that minimizes the distance between the auxiliary vectors obtained from observed data and from data simulated from the model.

sparsity, low reciprocity, and skewed degree distribution. In particular, the estimated model implies a tiered network structure characterized by the presence of a few highly interconnected core banks that intermediate in the market and the presence of many sparsely connected peripheral banks that almost exclusively trade with the core banks. Banks in the core typically have a structural liquidity deficit (investment opportunity) but large variances in liquidity shocks. On the other hand, peripheral banks typically have a structural funding surplus and experience small-scale shocks. Part of the network's tiered structure can be explained by banks' heterogeneous liquidity shocks. However, comparing the estimated model with a calibrated model that omits monitoring (but holds everything else equal) and with a restricted estimation shows that credit-risk uncertainty and peer monitoring are crucial in reinforcing the network's core-periphery structure: large money center banks are more intensively monitored by their lenders, and they in turn closely monitor their borrowers, leading to both lower bid and offer rates, as well as fueling their role as market intermediaries.

Second, the core-periphery structure of both the estimated and the observed lending network is stable across time. In particular, we find that bank pairs form long-term trading relationships that are associated with lower interest rates and improved credit availability. Problems pertaining to bank-to-bank uncertainty are small, as these relationship pairs engage in repeated peer monitoring and counterparty search that crucially depend on banks' persistent expectations about bilateral credit availability and conditions. In this respect, the findings indicate that bank-specific differences in funding and investment opportunities, as reflected in heterogeneous liquidity shock distributions, determine the bilateral trading opportunities among bank pairs and these, in turn, affect lending relationships in the interbank market. Specifically, on average banks with complementary shocks or a large variance of liquidity shocks profit from forming a bilateral lending relationship. However, our analysis shows that the multiplier effect that results from monitoring is necessary to generate bilateral stability and to replicate, by a magnitude similar to that observed in the data, the impact that relationship lending has on interest rates.

Third, our dynamic analysis reveals that adverse shocks to credit-risk uncertainty can suppress market activity for extended periods of time. The lending network shrinks because bilateral interest rates increase as a response to the higher perceived counterparty risk. Hence, interbank lending becomes less profitable relative to using the outside options (the central bank's lending and deposit

facilities), and recourse to the standing facilities replaces a number of trades. Moreover, in response to the shock and in expectation of higher uncertainty in the future, associated with lower profitability, banks invest less in peer monitoring. Negative feedback loops between lower levels of peer monitoring and search amplify this reduction, thereby preventing a faster market recovery. We also find that after the adverse shock, the lending network becomes less interconnected and more concentrated among a few banks (larger reciprocity and more skewed degree distribution) as those banks with extensive trading relationships stay in the market. In particular, bank pairs that face low bank-to-bank credit-risk uncertainty (due to private information acquired through previous monitoring) continue to lend to each other and, as a consequence, the average interest rate spread of granted loans decreases during the crisis period.

Fourth, the analysis of the estimated model shows that the central bank's interest rate corridor (the interest rate spread between its lending and deposit facilities) is a crucial determinant of interbank lending activity. In particular, we find that by increasing the corridor width, the central bank fosters interbank lending by directly reducing the attractiveness of the outside options, thereby increasing the potential surplus obtainable from bilateral interbank lending. However, we also document an indirect multiplier effect: since the increased expected surplus from interbank trading intensifies banks' monitoring and search efforts, these in turn act to further improve credit conditions and credit availability in the market, leading to more liquidity and a more efficient market usage. Moreover, we find that in response to an increase in the central bank's corridor width, the interbank lending network destabilizes as more loans are settled outside of established relationships (spot lending increases). Finally, under the new policy regime, loans associated with higher bank-to-bank uncertainty are settled and, as a consequence, both the market's interest rate spread (relative to the corridor center) and the cross-sectional variation of spreads increase.

The paper is structured as follows. Section 2 discusses the related literature. Section 3 introduces the economic model. Section 4 provides details on the estimation procedure, discusses the model's parameter estimates, and analyzes the relative fit in terms of various criteria. Section 5 analyzes the estimated model and studies policy implications, while Section 6 concludes.

2 STYLIZED FACTS AND RELATED LITERATURE

Interbank lending networks exhibit two stylized facts. First, interbank markets exhibit a sparse core-periphery structure whereby a few highly interconnected core banks account for most of the observed trades. Peripheral banks have a low number of counterparties and almost exclusively trade with core banks.⁴ Second, interbank lending is based on stable bilateral trading relationships that facilitate access to credit and offer better loan conditions.⁵ By explaining these two stylized facts using a model based on credit-risk uncertainty and peer monitoring, our paper is related to several strands of the literature.

First, the basic economic forces driving the proposed interbank lending model are credit-risk uncertainty, peer monitoring, and search frictions. Thereby, our paper is related to recent work by Afonso and Lagos (2015), who propose a search model to explain intraday trading dynamics in the spirit of over-the-counter models such as Duffie, Garleanu, and Pedersen (2005). Like these authors, we also build our dynamic model on bilateral bargaining and search frictions. However, Afonso and Lagos (2015) abstract from the role of bank default that was introduced by Bech and Monnet (2013). Neither model accounts for credit-risk uncertainty nor focuses on explaining the network structure of interbank markets and the endogenous formation of trading relationships. Moreover, since these models assume a continuum of atomistic agents where the probability of two banks being matched repeatedly is zero, there is no role for the emergence of long-term trading relationships.

On the other hand, building on the classical banking model of Diamond and Dybvig (1983), Freixas and Holthausen (2005), Freixas and Jorge (2008), and Heider, Hoerova, and Holthausen (2015) have focused on the role that asymmetric information about counterparty risk plays in the allocation of liquidity. In particular, Heider, Hoerova, and Holthausen (2015) show that informational frictions can lead to adverse selection and a market freeze with liquidity hoarding. In these models,

⁴For empirical evidence on the topological structure of interbank markets see, for instance, Soramäki, Bech, Arnold, Glass, and Beyeler (2007), May, Levin, and Sugihara (2008), and Bech and Atalay (2010) for the United States; Boss, Elsinger, Summer, and Thurner (2004) for Austria; Iori, Masi, Precup, Gabbi, and Caldarelli (2008) and Lux and Fricke (2012) for Italy; Becher, Millard, and Soramäki (2008) for the United Kingdom; Craig and von Peter (2014) for Germany; and van Lelyveld and in 't Veld (2014) for the Netherlands.

⁵The existence of interbank relationship lending has been documented by, among others, Furfine (1999), Furfine (2001), Ashcraft and Duffie (2007), and Afonso, Kovner, and Schoar (2013) for the United States; Iori, Masi, Precup, Gabbi, and Caldarelli (2008), Affinito (2012) for Italy; Cocco, Gomes, and Martins (2009) for Portugal; and Bräuning and Fecht (2012) for Germany.

however, interbank markets are anonymous and competitive, and hence the models abstract from the actual over-the-counter (OTC) structure where deals are negotiated on a bilateral basis and the realized credit conditions depend on heterogeneous expectations both about counterparty risk and credit conditions. The role of peer monitoring and private information that we consider a key driver of interbank lending has been highlighted by Broecker (1990), Rochet and Tirole (1996), and Furfine (2001). The literature, however, lacks a model of peer monitoring at the bank-to-bank level in an OTC market.⁶

Second, our paper is related to the growing literature on how financial networks are formed (see, for example, Gale and Kariv 2007; Babus 2013; in 't Veld, van der Leij, and Hommes 2014; Vuillemeij and Breton 2014; and Farboodi 2014).⁷ In particular, Babus (2013) shows that when agents trade risky assets over-the-counter, asymmetric information and costly link formation can endogenously lead to an undirected star network with just one intermediary. Farboodi (2014) develops a model that generates a core-periphery structure in which banks try to capture intermediation rents. Crucially, her model relies on the assumption that there are differences in investment opportunities (see also in 't Veld, van der Leij, and Hommes 2014). Our model confirms the importance of this type of bank heterogeneity for the emergence of a core-periphery structure, but credit-risk uncertainty and peer monitoring are the key drivers of persistent bilateral lending relationships that reinforce the core-periphery structure. In contrast to these studies that are concerned with the emergence of a static network, our paper also analyzes the lending network's dynamic behavior and focuses on the econometric analysis of structural network models (in particular, parameter estimation).⁸

Third, our findings are related to empirical studies analyzing the functioning of interbank markets during the 2007–2008 financial crisis. For the U.S. overnight interbank market, Afonso, Kovner, and Schoar (2011) provide evidence that concerns about counterparty risk play a larger role than

⁶Babus and Kondor (2013) consider information aggregation in OTC markets for a given network structure, where agents infer the asset's value based on observed bilateral prices and quantities from other transactions. In contrast, in our model of bank-to-bank uncertainty, banks engage in bilateral monitoring and do not learn about a counterparty's riskiness from other bilateral prices.

⁷The effects of the network structure on financial contagion has been studied, for instance, by Georg (2013); Gai, Haldane, and Kapadia (2011); Acemoglu, Ozdaglar, and Tahbaz-Salehi (2015); and Gofman (2014). We do not focus on contagion effects in this paper.

⁸Most of the literature on the estimation of network models discusses the estimation of statistical, reduced-form models. A recent attempt to calibrate a network model is presented by Gofman (2014), who matches the density, the maximum degree, and the number of intermediaries with those of the federal funds market, as reported by Bech and Atalay (2010).

liquidity hoarding (Acharya and Merrouche 2013) in explaining the disruption of interbank lending around the time of the Lehman Brothers’ bankruptcy. The dynamics of our estimated model confirm that shocks to counterparty-risk uncertainty can reduce lending activity for extended periods of time that are also accompanied by a more concentrated lending network. In this latter respect, Gabrieli and Georg (2014) provide empirical evidence on the network shrinkage in the euro money market during the 2007–2008 financial crisis.

Fourth, our paper is related to the literature on monetary policy. Theoretical contributions on implementing monetary policy in a corridor system with standing facilities in the context of competitive markets include Poole (1968), Whitesell (2006), and Berentsen and Monnet (2008). Kahn (2010) provides a nontechnical overview and evidence for monetary policy regimes in several countries. Our paper extends this literature by analyzing the effects of changes in the interest rate corridor on the structure of the lending network and the cross-sectional distribution of interest rates. In particular, our model suggests that increasing the corridor width incentivizes peer monitoring and private interbank lending. However, absent a view on the central bank’s preferences, we cannot make statements about the optimal corridor width (cf. Bindseil and Jablecki 2011; Berentsen and Monnet 2008).

3 THE INTERBANK NETWORK MODEL

We model the interbank lending market as a network consisting of N nodes with a time-varying number of directed links between them. Each node represents a bank and each link represents an unsecured interbank loan that is characterized by a loan amount and an interest rate. Time periods are indexed by $t \in \mathbb{N}$. Banks are indexed by i or j , with $i, j \in \{1, \dots, N\}$.

Each period, banks are subject to positive or negative liquidity shocks that affect the daily operations of their payment accounts (for example, clients that want to make payments). Banks wish to smooth these shocks by borrowing and lending unsecured funds from each other using an OTC market. An option outside the interbank lending market exists, as banks have unlimited access

to the central bank’s standing facilities with deposit rate \underline{r} and lending rate \bar{r} with $\bar{r} \geq \underline{r}$.⁹

Banks enter the interbank market with the objective of lending and borrowing funds to maximize expected discounted profits by: (i) choosing which banks to approach for bilateral Nash bargaining about interest rates, and (ii) setting bilateral monitoring expenditures to mitigate *uncertainty* about counterparty credit risk.

In the following subsections, we discuss the model’s structure, solve for banks’ optimal dynamic monitoring and search decisions, and specify an adaptive expectation mechanism to derive the model’s reduced form.

3.1 COUNTERPARTY-RISK UNCERTAINTY

Borrowing banks may default on interbank loans and—due to the unsecured nature of interbank lending—impose losses on lenders. Bank j ’s *true probability of default* at time t is denoted by $P_{j,t}$ and is derived as the tail probability of a random variable $z_{j,t}$ that measures the *true financial distress* of bank j ,

$$P_{j,t} := \mathbb{P}(z_{j,t} > \epsilon).$$

In particular, $z_{j,t}$ is constructed so that bank j is forced into default whenever $z_{j,t}$ takes values above some common time-invariant threshold $\epsilon > 0$. This threshold can be interpreted as either a minimum regulatory requirement or a level that seems sufficient to operate in the market. We focus on the case when $z_{j,t}$ is identically and independently distributed (*iid*) for each bank j with $\mathbb{E}(z_{j,t}) = 0$ and $\sigma^2 = \text{Var}(z_{j,t})$, such that there is no cross-section or time heterogeneity in banks’ true default probability.

Asymmetric information about counterparty risk (the riskiness and liquidity of a borrower’s assets) is seen as a major characteristic of financial crises that leads to inefficient allocations in

⁹This paper focuses on banks’ liquidity management and does not consider asset-liability allocation problems other than those associated with interbank lending and resorting to the central bank’s facility.

money markets (see Heider, Hoerova, and Holthausen 2015).¹⁰ Our focus is on the *uncertainty* about counterparty credit risk that underpins the interbank lending network structure and drives its dynamics. Asymmetric information problems arise because counterparty risk assessment is not based on the true default risk but merely on the *perceived probability of default* that bank i attributes to bank j at time t . This probability is denoted by $P_{i,j,t}$ and is obtained as the tail probability of a random variable $z_{i,j,t}$ that measures bank i 's *perceived financial distress* of bank j . The perceived financial distress $z_{i,j,t}$ is based on the true financial distress $z_{j,t}$ but contains an added component of bank-to-bank uncertainty that is modeled by the addition of an independent *perception error* $e_{i,j,t}$ so that

$$z_{i,j,t} = z_{j,t} + e_{i,j,t},$$

where $e_{i,j,t}$ is a random variable distributed according to some density, with $\mathbb{E}(e_{i,j,t}) = 0$ and $\text{Var}(e_{i,j,t}) = \tilde{\sigma}_{i,j,t}^2$. The perception error introduces bank-to-bank-specific assessments about the counterparty credit risk posed by the same borrower, bank j . That is, different banks may form different risk perceptions about the same borrower.

Since the exact distribution of the perception error $e_{i,j,t}$ is unknown to bank i , every bank is assumed to approximate the tail probability of the extreme event of default by the conservative bound provided by Chebyshev's one-tailed inequality,¹¹

$$\mathbb{P}(z_{i,j,t} > \epsilon) \leq \frac{\sigma_{i,j,t}^2}{\sigma_{i,j,t}^2 + \epsilon^2} = \frac{\sigma^2 + \tilde{\sigma}_{i,j,t}^2}{\sigma^2 + \tilde{\sigma}_{i,j,t}^2 + \epsilon^2} =: P_{i,j,t}.$$

Hence, both the bank's true risk profile and the additional uncertainty resulting from the perception error increase the perceived probability of default, which lender banks use to make their credit-risk assessment. The asymmetric information problem (characterized by a strictly positive perception-error variance $\tilde{\sigma}_{i,j,t}^2$) drives a wedge between the perceived probability of default and the true probability of default, even under the assumption that the perception error has a mean of zero.

¹⁰In this respect, William Dudley, President and CEO of the Federal Reserve Bank of New York, remarked: "So what happens in a financial crisis? First, the probability distribution [representing a creditor's assessment of the value of a financial firm] shifts to the left as the financial environment deteriorates Second, and even more importantly, the dispersion of the probability distribution widens—lenders become more uncertain about the value of the firm. ... A lack of transparency in the underlying assets will exacerbate this increase in dispersion." ("More Lessons from the Crisis", November 13, 2009), see <http://www.bis.org/review/r091117a.pdf>.

¹¹Instead of the Chebyshev bound, one can assume that the banks use a certain distribution to compute this probability. In this case, we just have to use the respective cumulative distribution function.

The evolution of the perception-error variance $\tilde{\sigma}_{i,j,t}^2$ is determined by the knowledge that bank i has about bank j 's default risk. This knowledge depends on factors such as the pair's past trading history and, in particular, the monitoring expenditure that bank i allocates to learning about bank j 's financial situation (the monitoring is discussed in more detail in the following section). Specifically, we assume that the bank-to-bank uncertainty $\tilde{\sigma}_{i,j,t}^2$ evolves over time according to autoregressive dynamics given by

$$\log \tilde{\sigma}_{i,j,t+1}^2 = \alpha_\sigma + \gamma_\sigma \log \tilde{\sigma}_{i,j,t}^2 + \beta_\sigma \phi_{i,j,t} + \delta_\sigma u_{i,j,t}, \quad (1)$$

where $\alpha_\sigma \in \mathbb{R}$, $\gamma_\sigma \in (0, 1)$, $\beta_\sigma \geq 0$, and $\delta_\sigma >$ are parameters; $\phi_{i,j,t}$ is a function of past bilateral trading intensity and the monitoring cost that measures the amount of *new information* that bank i collects about the financial situation of bank j in period t ; $u_{i,j,t} \sim \mathcal{N}(0, 1)$ is an *iid* shock to the counterparty-risk uncertainty. Moreover, we impose the restriction that $\beta_\sigma \leq 0$, and hence the added information gathered through monitoring and past interaction (weakly) reduces the perception-error variance. Due to the log specification, $\tilde{\sigma}_{i,j,t}^2$ follows a nonlinear process $\tilde{\sigma}_{i,j,t+1}^2 = \xi_{i,j,t}(\phi_{i,j,t}, \tilde{\sigma}_{i,j,t}^2) = \xi(\phi_{i,j,t}, \tilde{\sigma}_{i,j,t}^2, u_{i,j,t})$. Further, we can derive $\frac{\partial \xi_{i,j,t}}{\partial \phi_{i,j,t}} < 0$ and $\frac{\partial^2 \xi_{i,j,t}}{\partial \phi_{i,j,t}^2} > 0$, and hence our model dictates that there are decreasing returns to scale in information gathering.

Equation 1 is at the core of our model, as it determines the time-variation and cross-sectional heterogeneity in the bank-to-bank-specific perceived probabilities of default $P_{i,j,t}$. Conditional on these bank-to-bank perceived probabilities of defaults, banks negotiate the loan conditions.

3.2 BARGAINING AND EQUILIBRIUM INTEREST RATES

In the OTC interbank market, bank pairs bilaterally negotiate the specific loan terms. In the following description of the bargaining process, without loss of generality, let bank i be the potential lender bank that has a liquidity surplus and bank j be the potential borrower bank that has a liquidity deficit. From the viewpoint of bank i , lending funds to bank j at time t at a given bilateral equilibrium interest rate $r_{i,j,t}$ is a risky investment with a stochastic return,

$$R_{i,j,t} = \begin{cases} r_{i,j,t} & \text{with probability } 1 - P_{i,j,t} \\ -1 & \text{with probability } P_{i,j,t}, \end{cases}$$

where we assume that given a default, the loss is 100 percent. We further assume that bank i is risk neutral and maximizes its expected lending profit conditional on the perceived probability of default $P_{i,j,t}$. The expected profit per euro is given by

$$\bar{R}_{i,j,t} := \mathbb{E}_t R_{i,j,t} = (1 - P_{i,j,t})r_{i,j,t} - P_{i,j,t},$$

where \mathbb{E}_t denotes the expected value with respect to the perceived default probabilities. The expected surplus that lender bank i obtains from lending to borrower j is based on the difference between $\bar{R}_{i,j,t}$ and \underline{r} , the outside option for lenders (the interest rate for depositing funds at the central bank's standing facilities), but takes into account that this difference only goes to lender bank i if it is not in default. If it is in default (with true probability $P_{i,t}$) any cash flow is transferred to the liquidator. Hence, the expected surplus of lender i when lending to borrower j is given by $(1 - P_{i,t})(\bar{R}_{i,j,t} - \underline{r})$.

For the borrower bank j , the cost per euro when borrowing from lender bank i is simply given by the equilibrium interest rate $r_{i,j,t}$. The expected surplus relative to \bar{r} , the outside option for borrowing from the central bank's lending facility, takes into account the true probability that bank j will default and is given by $(1 - P_{j,t})(\bar{r} - r_{i,j,t})$.¹² Note that we implicitly assume that when lender bank i defaults, a solvent borrower j will still have to repay the principal and interest to the liquidator.

We follow the standard approach and assume that banks negotiate interest rates bilaterally and agree on the generalized Nash bargaining solution (see, for instance, Bech and Klee 2011 and Afonso and Lagos 2015 for similar applications to interbank markets). Written in terms of surplus relative to the outside option, the bilateral equilibrium interest rate between lender i and borrower j at time

¹²In the model, all banks have unlimited recourse to the central bank's standing facilities (specifically to the marginal lending facility) at any point in time. Thereby, we implicitly assume that all banks have sufficient collateral to back these operations (the euro area's national central banks provide liquidity under the marginal lending facility either as overnight repurchase agreements or as overnight collateralized loans). Moreover, holding the required collateral imposes a zero cost for all agents. At the margin, the central bank does not price banks' borrowing, as it assesses banks' riskiness as a sunk cost.

t then satisfies

$$r_{i,j,t} \in \arg \max_{\tilde{r}} \left((1 - P_{i,t}) \left((1 - P_{i,j,t}) \tilde{r} - P_{i,j,t} \underline{r} \right) \right)^\theta \left((1 - P_{j,t}) (\bar{r} - \tilde{r}) \right)^{1-\theta},$$

where the outside options for lenders (\underline{r}) and borrowers (\bar{r}) satisfy $\bar{r} \geq \underline{r}$. The parameter $\theta \in [0, 1]$ denotes the bargaining power of lender i relative to borrower j . As the exchange of funds is voluntary, the bilateral Nash bargaining problem is subject to the participation constraints $r_{i,j,t} \leq \bar{r}$ and $\bar{R}_{i,j,t} \geq \underline{r}$, and hence the central bank's interest rate corridor sets the upper and lower bounds for the interbank lending rates.¹³

Normalizing $\underline{r} = 0$ and denoting $\bar{r} = r$, as well as ignoring the multiplicative factors, the corresponding bilateral equilibrium interest rate satisfies equivalently $r_{i,j,t} \in \arg \max_{\tilde{r}} \left((1 - P_{i,j,t}) \tilde{r} - P_{i,j,t} \right)^\theta \left((1 - P_{j,t}) (r - \tilde{r}) \right)^{1-\theta}$, which we solve to obtain

$$r_{i,j,t} = \theta r + (1 - \theta) \frac{P_{i,j,t}}{1 - P_{i,j,t}}, \quad (2)$$

where the last term is a risk premium depending on the perceived default probability, $P_{i,j,t}$, that reflects the potential principal loss. The minimum interest rate that lender i is willing to accept is $r_{i,j,t}^{min} = P_{i,j,t} / (1 - P_{i,j,t})$, which is obtained from setting $\mathbb{E}_t R_{i,j,t}$ equal to the return of the outside option. Similarly, the borrower will not accept rates higher than $r_{i,j,t}^{max} = r$. Importantly, when the perceived default probability is sufficiently high, it is possible that the rate at which a bank is willing to lend is higher than the rate that the central bank charges for using its lending facility. In such circumstances, banks will not trade with each other, and borrowers will turn to the central bank instead of using the interbank market. In fact, it is possible that the interbank market disappears if lending is perceived to be too risky.

¹³In contrast to search models such as Afonso and Lagos (2015), our bilateral bargaining solution is derived under the assumption that the outside option for each loan is always the central bank's standing facilities. In contrast, in search models where two agents from a continuous population are randomly paired and allowed to bargain the terms of trade, each agent's outside options are determined by the expected future trading opportunities that may arise in the market. For our purpose of estimating a structural network model with endogenous counterparty selection, this approach is computationally infeasible, as the costs of obtaining the outside options (computing the value function) for our high dimensional problem are prohibitive in our simulation-based estimation procedure. In contrast to Afonso and Lagos (2015), our bilateral bargaining problem also incorporates an expected return, as the borrower may default on the loan and be unable to repay the principal amount to the lender; see also the bargaining problem in Bech and Monnet (2013).

Using the definition of the perceived probability $P_{i,j,t}$, we can rewrite the bilateral equilibrium interest rate as a function of the default threshold, the true financial distress variance, and the variance of the perception error as

$$r_{i,j,t} = \theta r + (1 - \theta) \frac{\sigma^2 + \tilde{\sigma}_{i,j,t}^2}{\epsilon^2}.$$

Taking the partial derivatives of this function gives $\frac{\partial r_{i,j,t}}{\partial \sigma} = \frac{(1-\theta)2\sigma}{\epsilon^2} > 0$ and $\frac{\partial^2 r_{i,j,t}}{\partial \sigma^2} = \frac{2(1-\theta)}{\epsilon^2} > 0$, and similarly $\frac{\partial r_{i,j,t}}{\partial \tilde{\sigma}_{i,j,t}^2} = \frac{(1-\theta)2\tilde{\sigma}_{i,j,t}}{\epsilon^2} > 0$ and $\frac{\partial^2 r_{i,j,t}}{\partial \tilde{\sigma}_{i,j,t}^4} = \frac{2(1-\theta)}{\epsilon^2} > 0$. Thus, the equilibrium interest rate increases with the uncertainty about counterparty risk. Note also that the second derivative is the same, so that the bilateral interest rate exhibits the same curvature in both dimensions.

The partial derivative of the expected return with respect to the perception-error variance is $\frac{\partial \bar{R}_{i,j,t}}{\partial \tilde{\sigma}_{i,j,t}^2} = -\frac{\partial P_{i,j,t}}{\partial \tilde{\sigma}_{i,j,t}^2} + \frac{\partial (1-P_{i,j,t})}{\partial \tilde{\sigma}_{i,j,t}^2} r_{i,j,t} + (1 - P_{i,j,t}) \frac{\partial r_{i,j,t}}{\partial \tilde{\sigma}_{i,j,t}^2} = -\frac{\epsilon(1+r)\theta}{(\epsilon^2 + \sigma^2 + \tilde{\sigma}_{i,j,t}^2)^2} < 0$. These terms show the channels through which increasing uncertainty about counterparty risk affects the expected return. First, increasing uncertainty about counterparty risk decreases $\bar{R}_{i,j,t}$ as $\frac{\partial P_{i,j,t}}{\partial \tilde{\sigma}_{i,j,t}^2} > 0$; hence loss due to default becomes more likely. Second, increasing uncertainty about counterparty risk increases the risk premium that is obtained if the borrower survives. However, the net effect is negative and thus the expected return decreases for a larger perception-error variance.

The preceding analysis reveals that the bilateral equilibrium interest rate under the asymmetric information problem, here parametrized by the perception-error variance, is not Pareto efficient. Indeed, we can compute the interest rate and expected return for the perfect information case where $\tilde{\sigma}_{i,j,t}^2 = 0$ (denoted by $r_{i,j,t}^{PI}$ and $\bar{R}_{i,j,t}^{PI}$, where the superscript *PI* stands for the perfect information case) and compare it with the asymmetric information case,

$$r_{i,j,t} - r_{i,j,t}^{PI} = \frac{(1 - \theta)\tilde{\sigma}_{i,j,t}^2}{\epsilon^2} > 0 \quad \text{and} \quad \bar{R}_{i,j,t}^{PI} - \bar{R}_{i,j,t} = \frac{\epsilon^2(1+r)\theta\tilde{\sigma}_{i,j,t}^2}{(\epsilon^2 + \sigma^2)(\epsilon^2 + \sigma^2 + \tilde{\sigma}_{i,j,t}^2)} > 0,$$

which gives the total reduction in (expected) surplus per euro of the loan due to the asymmetric information problem. This loss of surplus depends positively on the perception-error variance $\tilde{\sigma}_{i,j,t}^2$, which may be reduced by banks' peer monitoring efforts, as discussed in the next subsection.

3.3 MONITORING, COUNTERPARTY SELECTION AND TRANSACTION VOLUMES

Banks can engage in costly peer monitoring targeted at mitigating asymmetric information problems about counterparty risk. Therefore, let $m_{i,j,t} \in \mathbb{R}_0^+$ denote the expenditure that bank i incurs in period t for monitoring bank j . The *added information* that bank i acquires about bank j in period t is a linear function of the monitoring expenditure in period t and a loan, $l_{i,j,t} \in \{0, 1\}$, from bank i to bank j , enacted during trading session t ,

$$\phi_{i,j,t} = \phi(m_{i,j,t}, l_{i,j,t}) = \beta_\phi + \beta_{1,\phi} m_{i,j,t} + \beta_{2,\phi} l_{i,j,t}. \quad (3)$$

The added information affects the perception-error variance in future periods (see Equation 1). By allowing $\phi_{i,j,t}$ to be a function of both the loan indicator $l_{i,j,t}$ and monitoring efforts $m_{i,j,t}$, we distinguish between (costly) active information acquisition, such as creditworthiness checks, and freely obtained information, such as trust, built through repeated interactions. Monitoring efforts only affect the information about borrower risk, which influences the uncertainty about counterparty risk (the asymmetric information problem).¹⁴

Due to the OTC structure of interbank markets, bilateral Nash bargaining between any banks i and j in the market occurs only if these two banks have established contact. Therefore, we introduce a binary variable $B_{i,j,t}$ that indicates if bank i and j are connected at time t , so that bargaining as described in the previous subsection is possible. Specifically, we model $B_{i,j,t}$ as a Bernoulli random variable with success probability $\lambda_{i,j,t}$ that can be influenced by the search efforts of bank j directed toward lender i ,

$$B_{i,j,t} \sim \text{Bernoulli}(\lambda_{i,j,t}) \text{ with } \lambda_{i,j,t} = \frac{1}{1 + \exp(-\beta_\lambda(s_{j,i,t} - \alpha_\lambda))}, \quad (4)$$

where $s_{j,i,t} \in \mathbb{R}_0^+$ captures the search cost incurred by bank j (which has a liquidity deficit) when approaching lender i in period t . Hence, we assume loans are borrower-initiated in the sense that banks with a liquidity deficit approach potential lender banks for bargaining. Moreover, we impose

¹⁴Because we are interested in the role of monitoring on credit-risk uncertainty as the main driving force behind the observed interbank network structure and its dynamics, we deliberately focus only on this channel of monitoring and abstract from endogenous feedback effects between monitoring and risk-taking that also affect the true default probability (which is exogenously given in our model).

the conditions that $\beta_\lambda > 0$ and $\alpha_\lambda > 0$. For $\beta_\lambda \rightarrow \infty$ this function converges to a step function that corresponds to a deterministic link formation at fixed cost α_λ . For $s_{j,i,t} = 0$, we still have $\lambda_{i,j,t} > 0$, so even with no search costs there is still a positive probability that contact occurs, allowing for bargaining and a transfer of funds from bank i to bank j .

Once two banks establish contact and bilateral Nash bargaining about the interest rate is successful, interbank lending takes place. The amount of the granted loan $y_{i,j,t}$ is exogenously given by a nonlinear transformation of two random variables that follow a lender-bank and borrower-bank-specific distribution,

$$y_{i,j,t} = \min\{\zeta_{i,j,t}^i, -\zeta_{i,j,t}^j\} \mathbb{I}(\zeta_{i,j,t}^i > 0) \mathbb{I}(\zeta_{i,j,t}^j < 0), \quad (5)$$

where the random variable $\zeta_{i,j,t}^i \in \mathbb{R}$ can be interpreted as bank i 's liquidity shock (superscript i) realized at the time the transaction occurs between bank i and j . The transaction-specific liquidity shocks cannot be used for transactions with other banks in the same (or subsequent) period but must be smoothed instantaneously with the central bank or the respective counterparty at hand.¹⁵

We allow for bank-level heterogeneity of liquidity shocks and assume that $\zeta_{i,j,t}^i$ is independently and normally distributed with the bank-specific mean μ_{ζ^i} and variance $\sigma_{\zeta^i}^2$ parameters such that

$$\zeta_{i,j,t}^i | \mu_{\zeta^i}, \sigma_{\zeta^i}^2 \stackrel{iid}{\sim} \mathcal{N}(\mu_{\zeta^i}, \sigma_{\zeta^i}^2), \quad \text{where} \quad \mu_{\zeta^i} \sim \mathcal{N}(\mu_\mu, \sigma_\mu^2) \quad \text{and} \quad \log \sigma_{\zeta^i} \sim \mathcal{N}(\mu_\sigma, \sigma_\sigma^2),$$

and we allow for correlation between μ_{ζ^i} and $\sigma_{\zeta^i}^2$ through the parameter $\rho_\zeta := \text{Corr}(\mu_{\zeta^i}, \sigma_{\zeta^i}^2)$. For convenience, we assume (conditional) independence and normality of liquidity shocks, as this allows us to analytically compute part of the model's solution. This simple type of heterogeneity in the distribution of banks' liquidity shocks allows us to model size effects related to the scale of banks'

¹⁵This modeling choice follows the idea that upon contact each (ordered) pair of banks can exchange a stochastic pair-specific amount of funds which is exogenously determined by a (transaction-specific) realization from their (bank-specific) liquidity shock distributions. As a consequence of this modeling choice, a lender bank i may have several loans with different counterparties during the same time period ($\sum_j l_{i,j,t} > 1$). Moreover, lender bank i may also be borrowing during the same time period ($\sum_j l_{i,j,t} > 0$ and $\sum_k l_{k,i,t} > 0$) such that intermediation may arise where some banks act as both borrower and lender in the market (see Craig and von Peter 2014). Furthermore, reciprocal lending relationships within one period may occur ($l_{i,j,t} = l_{j,i,t} = 1$). In a previous version of the paper, we assumed a different sampling scheme similarly to Babus (2013) and Vuillemeys and Breton (2014) where at each instance each bank is paired with at most one counterparty (for example, pairing two banks randomly at each instance). For a given observed data frequency (in our daily analysis), we then aggregate the simulated data to a lower frequency to allow for nodes with multiple links. The sampling scheme we employ can be seen as a computationally less costly shortcut to sampling at a higher frequency.

businesses through larger variances that are drawn from a log-normal distribution. Moreover, this assumption allows us to account for structural liquidity provision or demand by some banks through a nonzero mean $\mu_{\zeta_{i,t}}$. The parameter ρ_{ζ} allows both effects to be correlated; for instance, some banks on average might supply small amounts of liquidity to the market (for example deposit-collecting institutions).

To keep track of all the loans in the interbank network, we formally define the binary link variable $l_{i,j,t}$ that indicates if an interbank loan between lending bank i and borrowing bank j at time t is granted (the extensive margin of credit) as

$$l_{i,j,t} = \begin{cases} 1 & \text{if } B_{i,j,t} = 1 \wedge r_{i,j,t} \leq r \wedge y_{i,j,t} > 0 \\ 0 & \text{otherwise.} \end{cases} \quad (6)$$

Hence, an established contact is only a necessary condition for a successful interbank loan to take place: upon a contact being made, funds are transferred if and only if the bargaining process is successful.¹⁶

Finally, since the volume of a granted loan $y_{i,j,t}$ is exogenously determined, matching is only affected by bank j 's search efforts, while for a sufficiently good risk assessment, the interest rate bank i offers is only directly affected by its monitoring efforts. Thus, we abstract from credit rationing on the intensive margin of credit (that is, lender banks reduce the amount of loans that they grant in response to an increase in perceived counterparty risk).

3.4 PROFIT MAXIMIZATION, OPTIMAL MONITORING, AND SEARCH

Each bank $i \in \{1, \dots, N\}$ faces the dynamic problem of allocating resources to monitor its counterparties and to choose which bank to transact with in order to maximize the expected discounted payoffs from interbank lending and borrowing net of search and monitoring costs. Formally, the

¹⁶The bargaining process fails if two banks are in contact but the bilateral equilibrium interest rate does not satisfy the participation constraints or if both banks are on the same side of the market, that is, both have positive or negative liquidity shocks.

infinite-horizon dynamic optimization problem of each bank is given by

$$\max_{\{m_{i,j,t}, s_{i,j,t}\}} \mathbb{E}_t \sum_{s=t}^{\infty} \left(\frac{1}{1+r^d} \right)^{s-t} \sum_{j=1}^N \left(\underbrace{l_{i,j,t} \bar{R}_{i,j,t} y_{i,j,t}}_{\text{lending}} + \underbrace{l_{j,i,t} (r - r_{j,i,t}) y_{j,i,t}}_{\text{borrowing}} - m_{i,j,t} - s_{i,j,t} \right), \quad (7)$$

where the expected discounted payoff is expressed in terms of the expected surplus compared to the outside options provided by the central bank, and the maximization is subject to the restrictions imposed by the structure laid down in subsections 3.1–3.3. The interest rate r^d is used for discounting future cash flows; in our model, the interest rate banks can earn when depositing funds at the central bank. The intertemporal optimization problem is operationalized by conditioning on the bilateral equilibrium interest rates, $r_{i,j,t}$, characterized in subsection 3.2. Hence, in this subsection these interest rates appear as a restriction on the optimization problem instead of one of the objective function's arguments.¹⁷

To solve the optimization problem using the calculus of variation, we impose appropriate smoothness conditions on the objective function and linearize part of the analytically intractable Euler equation for monitoring; see Appendix A for the details and derivations. We then obtain the optimal linearized bank-to-bank monitoring choice as the affine function,

$$m_{i,j,t} = a_m + b_m \tilde{\sigma}_{i,j,t}^2 + c_m \mathbb{E}_t \tilde{\sigma}_{i,j,t+1}^2 + d_m \mathbb{E}_t B_{i,j,t+1} + e_m \mathbb{E}_t y_{i,j,t+1}, \quad (8)$$

where the intercept and coefficients are functions of the structural parameters. The policy rule shows that bank i 's optimal monitoring expenditures directed toward bank j depend on the current state of bank-to-bank credit-risk uncertainty, the expected future uncertainty, the expected volume of the loan, and on the expected probability of being contacted by bank j .¹⁸

We obtain an analytical solution for the optimal level of bank-to-bank search. The solution

¹⁷Note that actual default does not enter banks' objective functions ($\bar{R}_{i,j,t} y_{i,j,t}$ not $R_{i,j,t} y_{i,j,t}$) nor their constraint functions. What matters in the model is only the (perceived) probability of default that enters the pricing of interbank loans, as in Equation (2). We do not incorporate actual bank default into the model because in the sample that we use for the parameter estimation, we do not observe any bank defaults. Moreover, actual bank default is not essential for understanding the basic mechanisms of peer monitoring, credit-risk uncertainty, and counterparty search that drive the observed market structure and its dynamics. Clearly, because there is no actual default event in the model, there is also no contagion through mutual credit exposure.

¹⁸Note that in our model we focus on bilateral interbank lending and the recourse to central bank facilities. Hence, the optimal monitoring decisions are based on interbank lending only, and do not reflect any other bilateral exposure between banks.

depends on bank j 's expected surplus $\Delta_{i,j,t} := \mathbb{E}_t[y_{j,i,t}(r - r_{j,i,t})I_{j,i,t}]$ when borrowing from bank i :

$$s_{i,j,t} = \begin{cases} s(\Delta_{i,j,t}) & \text{for } \Delta_{i,j,t}\lambda(s(\Delta_{i,j,t})) - s(\Delta_{i,j,t}) \geq 0 \\ 0 & \text{for } \Delta_{i,j,t}\lambda(s(\Delta_{i,j,t})) - s(\Delta_{i,j,t}) < 0. \end{cases} \quad (9)$$

Here, the interior solution with positive search levels is obtained from the analytical solution to the first-order condition (see Appendix A) as

$$s(\Delta_{i,j,t}) := 1/\beta_\lambda \log \left(0.5(\sqrt{\Delta_{i,j,t}\beta_\lambda(\Delta_{i,j,t}\beta_\lambda - 4)} + \Delta_{i,j,t}\beta_\lambda - 2)e^{\alpha_\lambda\beta_\lambda} \right), \quad (10)$$

for $\Delta_{i,j,t}\beta_\lambda(\Delta_{i,j,t}\beta_\lambda - 4) \geq 0$. The optimal search strategy hence shows that for a positive expected return net of search cost, the solution satisfies Equation (10), with $s(\cdot)' \geq 0$. Thus, search efforts increase in the expected surplus. Note that $\lambda(0) > 0$, so even without undertaking search efforts, two banks will eventually connect with each other and bargain about potential loan outcomes.

It is important to highlight that lender i 's monitoring level with respect to borrower j depends on the expectation of being contacted for a loan. Similarly, borrower j 's search effort with respect to lender i depends on the expected surplus that can be obtained from borrowing from bank i . This connection between monitoring and counterparty selection, linked by banks' profit expectations, generates an amplification mechanism that lies at the core of this model.

3.4.1 ADAPTIVE EXPECTATIONS

The optimal monitoring and search levels in Equations (8) and (9) depend on expectations about bilateral credit availability and conditions. We assume that in the interbank market each bank forms bank-specific *adaptive expectations* about the credit conditions at other banks.¹⁹ Following Chow (1989, 2011), the adaptive expectation of bank i concerning variable $x_{i,j,t}$, denoted by

¹⁹The adoption of adaptive expectations is justified in the first place by the fact that in many settings, there exists very strong econometric evidence supporting the adaptive expectations hypothesis against the rational expectations hypothesis (see, for example, Chow 1989, 2011). Specifically, Evans and Honkapohja (2001) show that in many ways adaptive expectations are the most rational forecasting method to use when the true data-generating process is unknown. This argument seems especially relevant for modeling decisions in a highly complex system such as an OTC trading network. Second, adaptive expectations are much easier to handle. Indeed, it is impossible to use the model's deterministic steady-state as an approximation point for perturbation methods (see Appendix A). This renders the rational expectations solution computationally impractical. On the contrary, since adaptive expectations are solely dependent on past observations, the numerical nature of the equilibrium point does not present extra difficulties.

$x_{i,j,t}^* := \mathbb{E}_t x_{i,j,t+1}$, follows an exponentially weighted moving average (EWMA),

$$x_{i,j,t}^* = (1 - \lambda_x)x_{i,j,t-1}^* + \lambda_x x_{i,j,t}, \quad (11)$$

where all variables are in deviation from the mean steady-state values. Banks use this forecasting rule for variables that are always observed by bank i ($\tilde{\sigma}_{i,j,t+1}$ and $B_{i,j,t+1}$). The parameter $\lambda_x \in (0, 1)$ determines the weight of the new observations at time t relative to the previous expectation.

However, a crucial implication of the opaque OTC structure of the interbank market is that a bank learns about credit conditions (that is, volumes $y_{i,j,t+1}$ and rates $r_{i,j,t+1}$) at *other* banks only when contact is made (information about credit availability and conditions at other banks is not publicly available). Our model incorporates this feature of decentralized interbank markets by assuming that bank i uses the following forecasting rule,

$$x_{i,j,t}^* = (1 - \lambda_x)x_{i,j,t-1}^* + \lambda_x B_{i,j,t} x_{i,j,t}. \quad (12)$$

Recall that $B_{i,j,t}(s_{j,i,t}) = 1$ denotes an “open” connection. Hence, new information about a counterparty is added to the expectation only if the banks have established contact in period t ; otherwise, the last forecast is not maintained but discounted by a factor $(1 - \lambda_x)$. Thus, if banks i and j are not in contact for many periods, their expectations converge to the mean steady-state values.

The formulation of the expectation mechanism completes the description of the model. Figure 1 summarizes the sequence of events taking place within one period. From the structural model, we obtain a reduced form that allows simulations from the parametric model under some given parameter vector; details on the reduced-form representation and stability conditions are provided in Appendix B.

4 PARAMETER ESTIMATION

We now turn to the estimation of the structural model’s parameters using loan-level data from the Dutch overnight interbank lending market. To estimate the parameters of the complex dynamic network model (nonlinearity and nonstandard distributions), we propose a simulation-based indirect

inference estimator that builds on an appropriate set of auxiliary statistics.

4.1 AUXILIARY STATISTICS AND INDIRECT INFERENCE ESTIMATOR

Following the principle of indirect inference introduced in Gourieroux, Monfort, and Renault (1993), we estimate the vector of parameters $\boldsymbol{\theta}_T$ by minimizing the quadratic distance between the auxiliary statistics $\hat{\boldsymbol{\beta}}_T$ obtained from the observed data X_1, \dots, X_T , and the average of the auxiliary statistics $\tilde{\boldsymbol{\beta}}_{TS}(\boldsymbol{\theta}) := (1/S) \sum_{s=1}^S \tilde{\boldsymbol{\beta}}_{T,s}(\boldsymbol{\theta})$ obtained from S simulated datasets $\{\tilde{X}_{1,s}(\boldsymbol{\theta}), \dots, \tilde{X}_{T,s}(\boldsymbol{\theta})\}_{s=1}^S$ generated under $\boldsymbol{\theta} \in \Theta$. Formally, the indirect inference estimator is thus given as

$$\hat{\boldsymbol{\theta}}_T := \arg \max_{\boldsymbol{\theta} \in \Theta} \left[\hat{\boldsymbol{\beta}}_T - \frac{1}{S} \sum_{s=1}^S \tilde{\boldsymbol{\beta}}_{T,s}(\boldsymbol{\theta}) \right]' \mathbf{W}_T \left[\hat{\boldsymbol{\beta}}_T - \frac{1}{S} \sum_{s=1}^S \tilde{\boldsymbol{\beta}}_{T,s}(\boldsymbol{\theta}) \right],$$

where Θ denotes the parameter space of $\boldsymbol{\theta}$ and \mathbf{W}_T is a weight matrix. Under appropriate regularity conditions, this estimator is consistent and asymptotically normal. In particular, consistency holds as long as, for given $S \in \mathbb{N}$, the auxiliary statistics converge in probability to singleton limits $\tilde{\boldsymbol{\beta}}_{T,s} \xrightarrow{p} \boldsymbol{\beta}(\boldsymbol{\theta}) \forall \boldsymbol{\theta}$ and $\hat{\boldsymbol{\beta}}_T \xrightarrow{p} \boldsymbol{\beta}(\boldsymbol{\theta}_0)$ as $T \rightarrow \infty$, where $\boldsymbol{\theta}_0$ denotes the model parametrization that has generated the data, while the so-called *binding function* $\boldsymbol{\beta} : \Theta \rightarrow \mathcal{B}$ that maps the structural parameters into the auxiliary statistics is injective. Convergence in probability is precisely ensured through the application of the law of large numbers for strictly stationary and ergodic data (see White 2001). Similarly, asymptotic normality of the estimator is obtained if the auxiliary statistics $\hat{\boldsymbol{\beta}}_T$ and $\tilde{\boldsymbol{\beta}}_{T,s}$ are asymptotically normal (see Gourieroux, Monfort, and Renault 1993). By application of a central limit theorem (see, for example, White 2001), the asymptotic normality of the auxiliary statistics can again be obtained by appealing to the strict stationarity and ergodicity of both the observed and simulated data.

The injective nature of the binding function is the fundamental identification condition which ensures that the structural parameters are appropriately described by the auxiliary statistics. This condition cannot be verified algebraically since the binding function is analytically intractable. However, identification will be ensured as long as the set of auxiliary statistics adequately describes both observed and simulated data. Hence, we select auxiliary statistics that provide a comprehensive characterization of the interbank market represented by the network of bilateral loans and the

associated loan volumes and interest rates. Specifically, in line with the estimation of dynamic models (see, for example DeJong and Dave 2006 and Ruge-Murcia 2007), we use the auto-covariance structure as well as higher-order moments, such as measures of skewness and kurtosis that are justified by the model's nonlinearity.

In addition to these standard auxiliary statistics, we base the indirect inference estimator on auxiliary statistics that specifically characterize the topological structure of the interbank lending network. In particular, since our model focuses on explaining the economic mechanisms behind the observed patterns of relationship lending and the sparse core-periphery structure, we include statistics that measure these characteristics. Therefore, we follow the large empirical literature on the structure of interbank lending networks and use key network statistics that are common in empirical analysis (see, for example, Jackson 2008; Bech and Atalay 2010). Moreover, we only include network statistics that are easy to compute, due to the large number of simulated networks in the estimation procedure.

First, we consider global network statistics. In particular, the *density*, defined as the ratio of the actual to the potential number of links, is a standard measure of a network's connectivity. A low density characterizes a sparse network with few links. *Reciprocity* measures the fraction of reciprocal links in a directed network. For the interbank market, this relates to the degree of mutual lending between banks. The *stability* of a sequence of networks refers to the fraction of links that do not change between two adjacent periods. Note that all three statistics are bounded between zero and one.

Second, we include bank-level (node-level) network statistics. The (unweighted) *in-degree* of a bank is defined as the number of lenders it is borrowing from, and the (unweighted) *out-degree* as the number of borrowers to which it is lending. We summarize this bank-level information using the mean and standard deviation of the (in-/out-) degree distribution as well as its skewness. The (local) *clustering coefficient* of a node quantifies how close its neighbors are to being a clique (complete graph). In the interbank network, this coefficient measures how many of a bank's counterparties have mutual credit exposures. We compute the clustering coefficients for directed networks as proposed by Fagiolo (2007) and consider the average clustering coefficient as an auxiliary statistic.

Third, we focus on simple bilateral network statistics that measure the intensity of a bilateral

trading relationship based on past lending activity during a rolling window. Similar to Furfine (1999) and Cocco, Gomes, and Martins (2009), we compute the number of loans bank i granted to bank j during the previous week and denote this variable by $l_{i,j,t}^{rw}$. We then compute a cross-sectional correlation between these relationship variables and loan outcomes at time t (the decision to grant a loan and interest rate). The first variable $\text{Corr}(l_{i,j,t}, l_{i,j,t-1}^{rw})$ is a measure of the bilateral stability of lending relations, while $\text{Corr}(r_{i,j,t}, l_{i,j,t-1}^{rw})$ is a proxy for the effects of relationship lending on interest rates.

We compute all the described network statistics for each lending network within the sequence of networks such that we obtain a sequence of network statistics associated with the sequence of networks. We then obtain the unconditional means, variance, and/or autocorrelation of these sequences as auxiliary statistics and base the parameter estimations only on the values of the auxiliary statistics. In Appendix C, we provide the formulae of the described network statistics.

Our estimator is based on a quadratic objective function with a diagonal weight matrix \mathbf{W}_T , as we refrain from using an asymptotically efficient weight matrix. This is because the inverse of the covariance matrix is only optimal under an axiom of correct specification. In addition, even under the correct specification, the (asymptotically) optimal weight matrix can lead to a larger variance of the estimator in finite samples. Moreover, for theoretical economic reasons, there are a number of auxiliary statistics that we wish to approximate better than others. As such, we adopt a matrix \mathbf{W}_T corresponding to an identity matrix, but the weight of the average degree (scaled density) and $\text{Corr}(l_{i,j,t}, l_{i,j,t-1}^{rw})$ are set to 10 and the weight of $\text{Corr}(r_{i,j,t}, l_{i,j,t-1}^{rw})$ is set to 50 because we want to match these characteristics particularly well. However, our results are qualitatively similar if we use an identity matrix as the weight matrix.

In all the estimations, we use $S = 24$ simulated network paths, each with a length of 4,000 periods, with the initial 1,000 periods burned to minimize dependence on the initial values (the effective sample size is 3,000 periods).²⁰ In the estimation, some of the structural parameters are calibrated as these are not identified by the data. For example, it is clear that several combinations of β_σ , $\beta_{1,\phi}$, and $\beta_{2,\phi}$ imply the same distribution for the data, and hence, also for the auxiliary

²⁰Our choice is motivated by computational considerations, as we parallelize the simulation of paths on a computer cluster.

statistics. The same implication applies for ϵ and σ . Further, we fix the common default threshold ϵ and the common true variance of the financial distress σ^2 to obtain an upper bound on the true probability of default of 0.01. We calibrate the corridor width to the average value of 1.5 percentage points observed in our sample period and set the discount rate to 1.75 percent per annum. The scaling parameter of the logistic function that approximates the step function when solving the model is set to 200.

4.2 DATA DESCRIPTION

The original raw data that we use in the estimation procedure comprise the daily bilateral lending volumes and interest rates realized in the overnight unsecured lending market among all Dutch banks. In particular, our empirical analysis is based on a confidential transaction-level dataset of interbank loans compiled by central bank authorities, based on payment records in the European large-value payment system TARGET2. This panel of Dutch interbank loans has been inferred by using a modified and improved version of the algorithm proposed by Furfine (1999) for the U.S. Fedwire system; for details on the dataset and methodology, see Heijmans, Heuver, and Walraven (2011) and Arciero et al. (2013).²¹

Our interbank loan-level dataset contains observations on daily bilateral volumes ($y_{i,j,t}$) and interest spreads ($r_{i,j,t}$) for the sample from February 19, 2008, through April 28, 2011 ($T = 810$ trading days). From these data, we construct the loan indicator $l_{i,j,t}$ that equals one if a loan from lender i to borrower j at day t is observed, and is zero otherwise. For computational reasons, we focus on overnight interbank lending among the 50 largest Dutch banks based on the frequency of their overnight trading (as both borrower and lender) throughout the entire sample period.²² As a

²¹The idea of Furfine-type algorithms is to match payment lags between bank pairs and identify interbank loans depending on the size of the initial payment, and size and date of candidate repayments. Compared to interbank lending data derived from the U.S. Fedwire data and payment systems of other countries, our dataset has three major advantages. First, TARGET2 payments have a flag for transactions related to interbank credit payments, which restricts the universe of all payments searched by the algorithm. Second, information about the actual sender and receiver bank is available. Unlike settlement banks, sender and receiver banks are the ultimate economic agents involved in the contract. In particular, the sender bank is exposed to the inherent counterparty credit risk that is at the core of our model. Third, and most important, euro-area interbank lending data derived from Furfine-type algorithms have been cross-validated with official Spanish and Italian interbank transaction-level data yielding type I errors of less than 1 percent. That is, less than 1 percent of all payments are incorrectly paired and classified as interbank loans (see Arciero et al. 2013 and Frutos et al. 2014).

²²The banks are consolidated at the bank holding company level, so intra-group traffic is ignored and dropped from the sample.

result, the data from which the auxiliary statistics are obtained consist of three $50 \times 50 \times 810$ arrays with elements $l_{i,j,t}$, $y_{i,j,t}$, and $r_{i,j,t}$. The arrays for $y_{i,j,t}$ and $r_{i,j,t}$ contain missing values if and only if $l_{i,j,t} = 0$.²³

Table 1 shows the key summary statistics of the data used in the analysis, with more detailed summary statistics provided in Appendix E. Note that: (i) the moments of bilateral volumes of granted loans are for values stated in (logarithm of) EUR millions; (ii) the moments of bilateral interest rates of granted loans are reported in percentage points per annum above the ECB deposit facility rate (the interest rate corridor’s lower bound); (iii) the daily interbank network is very sparse, with a mean density of 0.02 (on average, 1.04 lenders and borrowers) and low clustering; (iv) the distribution of interest rates, volumes, degree centrality, and clustering are highly skewed. It is also important to emphasize that the high autocorrelation of the density, the high stability of the network, and the positive expected correlation between current period lending and past lending activity can be seen as evidence of “trust” relations between banks, thus showing that past trades affect future trading opportunities. Similarly, the negative expected correlation between past lending activity and current interest rates provides evidence of lower perceived default risk that may result from monitoring efforts postulated by the proposed structural model.

Figure 2 presents the evolution of the daily network density, stability, average (log) volume, total volume, and the mean and standard deviation of the daily spreads over time during the sample period. From the plots, we see that the network density and total trading volume declined after Lehman’s failure on September 15, 2008 (indicated by the vertical red line). In economic terms, the total trading volume declines from about EUR 20 billion to EUR 10 billion. At the same time, the network stability and the daily cross-sectional standard deviation of interest rate spreads more than tripled. Moreover, the mean interest rate spreads of granted loans are close to the deposit facility as of October 2008, when the ECB introduced its fixed-rate full allotment policy. Further, the plots reveal that the data exhibit well documented end-of-maintenance period effects that we clean out in the construction of the auxiliary statistics by regressing each sequence of network statistics on end-of-maintenance period dummies before computing auxiliary statistics.

²³The dataset contains only loans of at least 1 million euros in volume, as typically banks with liquidity shocks below that amount do not go to the interbank market. Therefore, Equation (5) for the volumes of granted loans changes accordingly to $y_{i,j,t} = \min\{\zeta_{i,j,t}^i, -\zeta_{i,j,t}^j\} \mathbb{I}(\zeta_{i,j,t}^i \geq c) \mathbb{I}(\zeta_{i,j,t}^j \leq c)$, with $c = 1$ EUR millions.

4.3 ESTIMATION RESULTS

We now turn to the estimation results for the interbank network model. Table 2 shows the point estimates $\hat{\theta}_T$ and standard errors of the structural parameters using the auxiliary statistics reported in Table 4. Naturally, standard errors are not provided for calibrated parameters. For comparison with the indirect inference estimates, we also present θ^r , an alternative calibrated parameter vector, which equals $\hat{\theta}_T$ but restricts the effects of monitoring to zero ($\beta_{\phi,1} = 0$). By changing only one parameter of $\hat{\theta}_T$, we analyze the role of peer monitoring with a *ceteris paribus* argument. Table 2 also depicts the estimated parameter vector $\hat{\theta}_T^r$ of the restricted model ($\beta_{\phi,1} = 0$) to analyze the fit of the model without monitoring when the other parameters are re-estimated and fully determined by the data.

The parameter estimates $\hat{\theta}_T$ reported in Table 2 are interesting in several respects. First, the autoregressive log-variance process's relatively large and significant intercept can be seen as evidence for high levels of prevailing bank-to-bank uncertainty. Also, the autoregressive parameter γ_σ is estimated to be 0.66, indicating that in the absence of new information, there is a positive autocorrelation in bilateral credit-risk uncertainty. The estimate of the scaling parameter δ_σ is positive and significant, indicating that shocks to credit-risk uncertainty are important drivers of bank-to-bank uncertainty. Moreover, $\beta_{\phi,1}$, the estimated coefficient that determines the effect that peer monitoring has on the additional information about credit risk, is positive and statistically significant. Hence, we find evidence that monitoring is a significant factor in reducing the prevailing bank-to-bank uncertainty regarding counterparty risk. On the other hand, the estimated coefficient that determines a transaction's effect is close to zero and statistically insignificant. This result suggests that credit-risk uncertainty is not mitigated by repeated transactions, but depends on monitoring efforts.²⁴

Second, the positive estimates for α_λ and β_λ show that counterparty search is a crucial feature in the formation of interbank networks. In particular, the large and significant estimate for β_λ is 73, which suggests that links are not randomly formed, but rather are strongly influenced by banks'

²⁴The restricted model's estimation results show that without monitoring, the effects of past transactions on the reduction of bank-to-bank uncertainty is stronger. Hence, the restricted model attributes part of the effects of monitoring to the mere existence of past trading activity.

search for preferred counterparties. With such large scaling, the logistic function mimics a step function quite well. The significant role of endogenous counterparty selection also highlights the effect of expected profitability (expected loan volumes and interest rates) on the search decisions. In this respect, the positive point estimate of 0.85 for λ^y indicates persistent expectations about available bilateral loan volumes. Similarly, the estimated value of 0.93 for λ^B indicates a strong persistence in the expectation of being contacted by a specific borrower. These persistent expectations eventually contribute to the high persistence of bilateral trading relationships. The estimated value for λ^r is considerably lower (0.40), suggesting that new information about bilateral interest rates is more heavily weighted in the expectation formation process, compared to expectations about volumes and contacts which are relatively more persistent. On the other hand, the changes in bank-to-bank credit-risk uncertainty immediately feed into expectations, as the 0.03 estimate for $\lambda^{\tilde{\sigma}}$ indicates. Clearly, the model without monitoring does not include the parameters λ^B and $\lambda^{\tilde{\sigma}}$, which affect the monitoring decisions only through the optimal monitoring policy rule.

Third, the distribution's estimated values of the hyper-parameters of the distribution that characterize banks' individual liquidity shock distributions point toward significant heterogeneity. The estimated log normal distribution implies that there are a few banks with very large liquidity shock variances that are very active market players. Moreover, the notion that some banks structurally provide or demand liquidity is supported by the positive estimate of the mean's variance parameter. Note also the estimated negative correlation parameter, which indicates that banks with a small liquidity shock variance typically have a positive mean.²⁵ We discuss the role of bank heterogeneity in more detail in Section 5.

In Table 3, we report the coefficients of the linear policy rule for the optimal monitoring levels as implied by the estimated parameters (monitoring is expressed in deviations from steady-state values). It is particularly noteworthy that the optimal monitoring level toward a particular bank depends positively on the expected probability of being approached by this bank to borrow funds during future trading sessions, $\mathbb{E}_t B_{i,j,t+1}$. Indeed, this positive coefficient and the significantly positive effect of search on link formation (endogenous counterparty selection) create the connection between

²⁵Interestingly, the estimation results of the restricted model without monitoring do not exhibit this negative correlation; instead, there is a larger variance in banks' mean and standard deviation parameters.

monitoring and search as the source of persistent trading relationships. Moreover, the current state of credit-risk uncertainty positively affects monitoring during the current period. Higher expected future uncertainty, however, reduces these efforts as the expected profitability of interbank lending declines. The positive coefficient on the amount of granted loans shows that banks prefer to monitor those counterparties with whom they expect to trade larger volumes. This finding is intuitive, since the surplus that can be generated by reducing credit-risk uncertainty is larger. Hence, monitoring reacts positively to expectations of increased profits in the future, similar to banks' optimal search decision.

The estimated policy rules for peer monitoring and search imply that shocks to interbank trading profitability lead to an endogenous multiplier effect that works as follows. Suppose there is a positive shock to the bilateral loan (or similarly a positive shock to the link, or a negative shock to the credit-risk uncertainty). In response, banks' expected profitability increases, and banks increase their monitoring and search efforts. As a consequence, more loans are granted and interest rates decrease. These developments feed into banks' expectations about spreads and bilateral link probabilities, which further promotes monitoring and search. As a consequence, the multiplier effect of monitoring and endogenous counterparty selection further drives up the link probability and reduces interest rates. Thus, the initial shock to interbank profitability is reinforced by the interrelationship between control variables, outcomes, and state variables. This basic amplification mechanism is at the core of our model and can explain several features of the observed interbank network that we discuss next.

5 MODEL ANALYSIS

In this section, we use the estimated structural model to study the effects of key frictions on the network structure. Our analysis focuses on assessing the role of private information, gathered through peer monitoring and repeated interactions, in shaping the network of bilateral lending relationships and associated interest rates and volumes. Moreover, we use the model to analyze the effect that changes in the central bank's discount window have on the interbank lending structure.

5.1 COMPARISON OF AUXILIARY STATISTICS

We first analyze the model’s fit, along with the observed and simulated values of the auxiliary statistics under the estimated structural parameter $\hat{\theta}_T$. We benchmark our estimated model against an alternative model parametrization θ^r , where the effects of monitoring on the perception-error variance are restricted to zero ($\beta_{\phi,1} = 0$). By focusing on the monitoring channel, but keeping all other things equal (in particular, the parameters related to banks’ liquidity shock distribution and search technology), we evaluate the role of peer monitoring on the network structure and associated bilateral credit conditions from a *ceteris paribus* perspective. Moreover, we compare the fit of the full model to the restricted but re-estimated model without monitoring ($\beta_{\phi,1} = 0$), where all the other parameter values are determined by the data (parameter vector $\hat{\theta}_T^r$).

Table 4 shows how the estimated structural parameter vector $\hat{\theta}_T$ produces an accurate description of the data when compared to the alternative calibrated parameter vector θ^r without monitoring. First, note the remarkable improvement in model fit compared to the calibrated example. This is brought about by the indirect inference estimation, as judged by (i) the value of the (log) criterion function that is about 54 times smaller for the estimated model, and (ii) the comparison between auxiliary statistics obtained from the observed data, data simulated at the calibrated parameter, and data simulated at the estimated parameters. For instance, the Euclidean norm and the sup norm of the difference between observed and simulated auxiliary statistics are about 3.5 and 5 times larger, respectively, under the calibration without monitoring. Also, when compared with the restricted estimated model without monitoring (parameter vector $\hat{\theta}_T^r$), we find that the overall fit of the estimated model with monitoring provides a better description of the observed data, with the objective function value being only 0.62 as large and the Euclidean and sup norm of the distance between the observed and simulated auxiliary statistics being only 0.83 and 0.59 times as large, respectively.

A closer look at the individual auxiliary statistics confirms the importance of the peer monitoring channel for replicating the network structure and reveals several interesting features of the estimated model.²⁶ First, it is important to highlight the significant improvement in the fit of the density

²⁶In the following, we refer to the estimated model as the unrestricted model characterized by $\hat{\theta}_T$ (that is, the estimated model with monitoring).

compared to the calibrated example. In fact, with a density of about 0.02, the estimated model matches the sparsity of the Dutch interbank network very well. Hence, only a few bank pairs trade in the market on a daily basis. Likewise, the proposed structural model provides a very accurate description of the network’s high stability, with a value of 0.98. Similarly, with a small value of 0.03, the average clustering coefficient matches the data very well and is a considerable improvement over the calibrated model. Moreover, the estimated model implies that about 6.3 percent of all links are reciprocal, compared to 8.2 percent in the observed data.

Second, a comparison of the observed and simulated auxiliary statistics shows that the model well replicates the first three moments of the observed degree distribution.²⁷ In particular, the estimated model generates a high positive skewness of both the in-degree and out-degree distribution (compare the respective simulated skewness of 2.4 and 2.3 with the observed skewness of 2.8 and 2.4, respectively). Similarly, the standard deviation of both degree distributions are quite accurate, with respective values of 1.7 and 1.7 compared with the observed counterparts of 1.8 and 1.6. Figure 3 plots the simulated (marginal) in-degree and out-degree distributions under the estimated model parameters. The figure is the result of a Monte Carlo (MC) analysis based on 5,000 different networks, each with $T = 25$. About 65 percent of all banks have no (zero) trading partners on a daily basis (isolated vertexes); that is, they do not lend or borrow in the market. Moreover, about 60 percent of active banks have at most two borrowers and two lenders. At the same time, both degree distributions have a very long right tail indicating that there are few banks that borrow and lend from many other banks. Yet it is very rare for banks to have more than 10 counterparties on a daily basis—the relative frequency is below 1 percent.

To illustrate the basic network topology, Figure 4 depicts the observed interbank network along with a network simulated from the estimated model with monitoring. The figure shows the sparse and concentrated market structure—a few banks at the center of the network trade large volumes on either side of the market (the scale of the nodes relates to lending and borrowing volume). The visualization also highlights the skewed degree distribution of the observed and simulated network that is one key stylized fact of interbank markets. In particular, large banks in the core have multiple

²⁷The density is just a rescaled version of the average degree centrality; we did not include the density in the estimation but show it for convenience in Table 4.

counterparties, while small banks typically have few trading partners and are typically connected with banks in the center of the network.

Comparing the estimated auxiliary statistics with those obtained from the calibrated model θ^r without monitoring shows that monitoring is an important factor in explaining the basic topology of the observed lending network. In contrast to the estimated model with monitoring, the calibrated model fails to specifically match the network’s skewed out- and in-degree distributions, with simulated values of 0.45 and 0.33, respectively (note that banks’ liquidity shock distributions and all other parameters are held constant). In fact, the estimated model parameterization without monitoring $\hat{\theta}_T^r$ also fails to generate a skewed degree distribution close to the observed one, with out- and in-degree skewness of 1.36 and 1.40, respectively, although all parameters are fully determined by the data. Indeed, as we discuss in detail in the next section, the amplification mechanism of peer monitoring and counterparty selection reinforces the tiered market structure and generates a highly skewed degree distribution.

Third, and key to our analysis, the estimated structural model is able to generate patterns of relationship lending where banks repeatedly interact with each other and trade at lower interest rates. In particular, the positive correlation of 0.60 between past and current bilateral lending activity, that is, the measure of the stability of bilateral lending relationships, matches the observed value of 0.64 very well. Moreover, the model generates a negative correlation of -0.12 between interest rates and past trading (compared with -0.07 for the observed data). As reported in Table 3, monitoring efforts positively depend on the expectation of being approached by a specific borrower. Once a contact between two banks is established, banks positively adjust their expectations and increase monitoring. This greater monitoring effort has a dampening effect on the bilateral interest rate level and thereby makes borrowing more attractive, leading to increased expectations about a contact.

The role of bank-to-bank peer monitoring as the crucial driver behind the observed dynamic structure of the interbank market is also confirmed by comparing the fit of the auxiliary statistics simulated under the calibrated parameter with those of the estimated parameter. Clearly, in the calibrated example where there is no role for monitoring, the stability of bilateral trading relations is low (0.23), and past trading has no effect on current prices, as the effect of trading activity in reducing uncertainty ($\beta_{\phi,2}$) is small and insignificant. In contrast, the estimated model without

monitoring generates some relationship lending (-0.16), as the estimated value of $\beta_{\phi,2}$ is larger than in the calibration without monitoring. However, in the calibrated model, the simulated values for the stability of bilateral trading relationships are smaller (0.43), compared with the observed and simulated values of the full model (0.64 and 0.60 , respectively), highlighting the importance of the monitoring channel for the persistence of bilateral trading relationships in the market.

Moreover, our estimated model with monitoring—similarly to the estimation results for the restricted model—replicates rather well the mean and skewness of the distribution of (log) volumes of granted loans. Also, the standard deviation points toward heterogeneity in bilateral loan amounts, although the simulated value is not as large as the observed value. The distribution of the potential bilateral volumes depends on the bank-specific liquidity shocks in Equation (5). However, the decision to lend is endogenous, and hence the distribution of granted loans also depends on other model parameters. Note also that the estimated model does a worse job in explaining the observed average interest rate level, while it nicely captures the cross-sectional standard deviation of spreads that in our model is related to heterogeneous counterparty risk perceptions. Further, the skewness of the cross-sectional interest rate distribution has the correct sign but is twice as large as the observed value.²⁸

Finally, we find that our estimated model is able to generate some autocorrelation in the density (0.25) and the average interest rate of granted loans (0.24), in contrast to the average volume of granted loans. Clearly, the estimated values are not as high as the observed values (0.81 and 0.97 , respectively). However, there are no common factors in the model, and all shocks are *iid*. The only persistent processes are at the bank-to-bank level: credit-risk uncertainty and the bank-to-bank-specific expectations. Hence, the generated autocorrelation in these aggregate figures results from the same banks trading with each other in subsequent periods. Similarly, the model also generates a negative correlation between the density and the stability, and a positive correlation between density and average spreads. Thus, when there are fewer loans granted, the average interest-rate spread of these loans decreases. In our model, this happens because when counterparty-risk uncertainty is high, only bank pairs with low uncertainty (and hence low spreads) continue to trade.

²⁸Recall that the model abstracts from any bank heterogeneity beyond differences in liquidity shocks; in particular, differences in balance sheet strength or heterogeneous outside options. Moreover, in the current model there is no room for excess liquidity that might affect the level of interest rates.

In Appendix D, we document the network structure’s comparative statics to further analyze the role of several structural parameters related to credit-risk uncertainty and monitoring.

5.2 BANK HETEROGENEITY AND LENDING RELATIONSHIPS

In our model, heterogeneous liquidity shock distributions are the only source of bank heterogeneity. Yet these shocks are important in determining the exogenous volumes of granted loans. As banks’ monitoring and search efforts depend on expected loan volumes, the heterogeneous liquidity shock distributions determine the distribution of the multiplier effects from monitoring that are crucial in matching the basic network structure of the interbank market, such as the high skewness of the degree distribution as described in the previous subsection. In our model, the distribution of liquidity shocks in the banking system is characterized by the probabilistic structure described in Section 3.

Figure 5 plots the joint distribution of the bank-specific mean μ_{ζ^i} and the standard deviation σ_{ζ^i} of the liquidity shocks, as implied by the estimated structural parameters $\hat{\mu}_\mu = 0$, $\hat{\sigma}_\mu = 1.99$, $\hat{\mu}_\sigma = 1.94$, $\hat{\sigma}_\sigma = 1.98$, and $\hat{\rho}_\zeta = -0.78$. First, most probability mass is located around $\mu_{\zeta^i} = 0$ and at small values of σ_{ζ^i} . Hence, the median bank has small liquidity shocks that on average are about zero. Second, the distribution of μ_{ζ^i} is more dispersed for low values of σ_{ζ^i} . Thus, for banks with a small variance parameter of the liquidity shock distribution (small banks), there is higher heterogeneity with respect to their mean parameter μ_{ζ^i} . Third, the contour plot reveals that the distribution has a parabolic form. In particular, small banks with very small-scale liquidity shocks typically tend to have a liquidity surplus, while banks with very large-scale shocks typically have a negative mean, indicating a liquidity deficit. This relationship is driven by the correlation parameter ρ_ζ that we estimate to be -0.78 . Finally, the long tail in the dimension of σ_{ζ^i} shows that just a few banks have very large liquidity shock variances.

The estimated bank heterogeneity has important consequences for pairwise credit availability and conditions, as well as for search and monitoring expenses. In Figure 6, we show the interbank activity during one five-day business week for 50 randomly drawn liquidity shock parameters (associated with 50 banks). Each bank is indicated by a black dot, and its position in the μ_ζ - σ_ζ plane is given by the values of the bank-specific mean and standard deviation parameters $(\mu_{\zeta^i}, \sigma_{\zeta^i})$. The figure reveals that small banks (small liquidity-shock variance) typically provide liquidity to the interbank

market, particularly to big banks (those that on average have a positive demand for liquidity) or small banks with complementary liquidity shocks.²⁹ Market intermediation emerges as big banks (money-center banks) simultaneously act as lenders and borrowers. For small banks, it is most efficient to trade with big banks that have large liquidity shocks than with banks with small liquidity shocks. Moreover, big banks form a tightly interconnected core where each member of the core has reciprocal lending relationships (solid blue lines) with other core banks (see the core-periphery analyses by Craig and von Peter 2014 and van Lelyveld and in 't Veld 2014). Clearly, on average big banks trade larger loan volumes than small banks as a result of their larger-scale liquidity shocks.

We next present more rigorous Monte Carlo (MC) evidence to analyze the role of bank heterogeneity as the fundamental source of persistent trading opportunities. For this purpose, we simulate 5,000 network paths and for each draw sort the lender banks in increasing order according to their variance parameter σ_{ζ^i} and sort the borrower banks according to their mean parameter μ_{ζ^i} in increasing order. Hence, we compute the order statistics of both parameters. We then simulate for each draw 25 periods and compute the mean link probability, mean volume, and spreads of granted loans as well as the mean search and monitoring efforts between the lender's order statistics and the borrower's order statistics of all possible bank pairs.

Figure 7 shows the results of the MC analysis. Panel (a) depicts the mean granted-loan volumes for different bank pairs. In particular, we see that banks with a structural liquidity deficit (on the left of the horizontal axis) are borrowing larger amounts than banks with a structural liquidity surplus (on the right of the horizontal axis). Both types of banks borrow larger volumes from big banks with a large variance parameter (on the top of the vertical axis). Due to the negative correlation parameter ρ_{ζ} , banks with a low-order statistic $\mu_{\zeta^{(i)}}$ are typically big banks, and thus borrowing volumes with other big banks (with large $\sigma_{\zeta^{(i)}}$) are high. Similarly, the mean traded-volumes are low for banks with a structural liquidity surplus and lender banks with a small-scale variance parameter—see the blue region in Panel (a).

As exogenously determined by the distribution of liquidity shocks, the distribution of loan volumes affects the monitoring decisions that eventually affect the prices at which bank pairs trade

²⁹This result is in line with similar empirical findings by Furfine (1999) and Bräuning and Fecht (2012), among others, that small banks are net lenders in the interbank market.

liquidity (see Panels (c) and (e)). Those bank pairs that can exchange large loan amounts (either because they have a large liquidity shock variance or because on average they have complementary shocks) engage in more monitoring activity and trade at lower spreads (see the parabolic-shaped contour plots). Again, we see that the very large banks engage in high monitoring efforts and trade with each other at very low interest rates (up to 40 basis points lower than high-spread pairs). Hence, these core banks are not only highly interconnected, but the credit-risk uncertainty among these banks is very low (Panel (f)). Due to the interrelationship between monitoring and search, low-interest regions in the figures correspond to bank pairs where search levels are high, leading to high probabilities of successful linkages (see Panel (b)). Moreover, borrowers with a structural liquidity deficit obtain larger loan volumes at lower prices when borrowing from large banks compared with small banks. This discrepancy further highlights the role that intermediation plays in the estimated model. Intermediaries have less credit-risk uncertainty about their borrowers due to higher monitoring intensities, and in turn borrowers have lower credit-risk uncertainty about intermediary banks because lenders direct monitoring efforts toward those borrower banks. Hence, this behavior gives rise to the network’s tiered structure, which results from differences in liquidity shocks, reinforced by the presence of credit-risk uncertainty and peer monitoring, leading to different interest rates.³⁰

5.3 DYNAMIC RESPONSES TO CREDIT RISK UNCERTAINTY SHOCKS

In this section, we analyze how the dynamics of the estimated network model are affected by shocks to the perception-error variance. To account for the uncertainty about the precise latent liquidity shock distributions, we perform a simulation study by first drawing the properties of each bank (as described by the parameters μ_{ζ^i} and σ_{ζ^i}) and then calculating a set of key network statistics for 25 time periods. This procedure is then repeated in a Monte Carlo setting with 5,000 replications. In all the simulated structures, we impose a large positive shock to the perception-error variance in period $t = 4$ (thus affecting the perception-error variance in $t = 5$) to investigate how our key network statistics react to increases in credit-risk uncertainty.

³⁰Fecht, Nyborg, and Rocholl (2011) document that the price that banks pay for liquidity depends on the distribution of liquidity across banks.

The solid lines in Figure 8 depict the mean responses across all network structures to an extreme 10 standard deviation shock in credit-risk uncertainty; that is, we impose $u_{i,j,4} = 10 \forall i, j$. In this figure, the interquartile range (dotted lines) essentially reflects the uncertainty about the exact network structure as described by the unobserved liquidity shock distributions. For instance, the interquartile range of the mean network density is between 0.014 and 0.023, and the mean is about 0.019, depending on the precise network structure.³¹ In the top panel, we show that at the time of the shock to the credit-risk uncertainty, the network density drops by more than 75 percent. Both the density and total volume remain at low levels, and 20 trading days after the shock they still remain at only 50 percent of their pre-crisis values. Moreover, the log of total transaction volume plummets by more than 50 percent as a result of reduced trading activity. At the same time, we observe an increase in the average (log) volume of granted loans compared with pre-shock loan levels and an increase in the network stability one period after the shock. Similarly, both in-degree and out-degree distributions become more positively skewed, and there is over a two-fold increase in reciprocity.³² Hence, the network shrinks and trading becomes more concentrated among the highly interconnected core banks.

These changes are driven by the fact that in the aftermath of the shock, some bank pairs that had been actively trading cease this activity amid deteriorating risk assessments of borrowers. As the implied interest rate spreads explode, lending in the interbank market becomes unattractive for some pairs compared with the outside option. These loans are substituted by increased recourse to the central bank's standing facilities (not shown), which moves inversely to the density and total transaction volume in the interbank market. In fact, the increased average loan volume shows that for $t = 5$, a large fraction of trading bank pairs exchange larger volumes (due to their size and/or complementarity of liquidity shocks). As discussed in the previous section, these are bank pairs where monitoring is particularly profitable and bank-to-bank uncertainty is low, rendering interbank lending more attractive than the outside option, even after the shock. Yet, those trades that do occur also are associated with increased spreads due to higher uncertainty; the average spread of granted volumes increases by about 6 basis points right after the shock. Thus, the compositional

³¹For any fixed structure of liquidity shocks, the interquartile range is much tighter around the mean response.

³²The lower bound remains at zero because for some network structures interbank lending breaks down completely, leading to zero reciprocity.

effects do not immediately outweigh the uncertainty-induced increases in interest rates. However, about two periods after the shock, the average spread of the interbank trades that do occur return to the initial pre-shock levels, and a further decrease can be observed until about period 10 when the average rate of traded loans is below the pre-shock level. A similar pattern can be observed for the cross-sectional standard deviation of interest rates. While it falls to 0.11 as the shock hits, it decreases to about 0.09 in period 10 when the mean spreads are lowest, and then for an extended period of time rises to a value higher than pre-shock levels.

Figure 9 depicts how the impulse responses for the banks' expectations and control variables act as crucial drivers for the changes in the observable network statistics. Again, the solid line refers to the mean and the dotted lines refer to the interquartile ranges that represent the uncertainty about the latent network structure. The top left panel shows how the mean credit-risk uncertainty induced by the shock peaks in period five. Clearly, the increase in the mean credit-risk uncertainty translates into an increase in the mean expectations about future credit-risk uncertainty that displays similar behavior, although at lower values. As a consequence of the higher expected uncertainty after the shock (that directly translates into higher bilateral equilibrium rates), the expected profitability of interbank borrowing decreases as the spread that can be earned in the interbank market compared to discount window borrowing declines. This lower degree of profitability leads borrower banks to invest less in counterparty search, further bringing down trading in the interbank market. The impaired funding conditions due to higher credit-risk uncertainty only feed gradually into borrowers' expectations about interbank profitability, as borrowing banks only update their expectations once they are in contact with a lender. Therefore, the mean search effort by borrowers gradually declines until it reaches a minimum in period 10. Moreover, this reduced search effort is reflected in lenders' expectations about future contacting probabilities, which gradually decline from period 5 onward until the end of the plotted sample (although the decrease in the mean expectation is arguably small).

Moreover, as a response to the increased perception-error variance, banks adjust their monitoring expenditures from about 4,500 euros on average (per bank-pair) downward to 2,000 euros. This decrease, which contributes to the prolonged period of interbank trading inactivity that prevents a fast market recovery, is driven by several channels. First, from the estimated linear policy rules, we

find that banks increase monitoring as a response to higher credit-risk uncertainty. However, at the same time, they decrease peer monitoring to adjust to future expected uncertainty. Because the estimated exponentially weighted moving average (EMWA) parameter is low, these expectations closely follow the actual credit-risk uncertainty that has quite persistent dynamics. In sum, the negative effect of future uncertainty dominates such that the overall mean effect of this large 10 standard deviation shock is negative. Second, due to lower search efforts, the gradual decrease in the probability of expected future contact further dampens banks' monitoring expenditures and prevents the interbank market from making a faster recovery. In Figure 9, we plot the mean values of bank-to-bank-specific expectations and control variables.³³

5.4 MONETARY POLICY ANALYSIS: THE INTEREST RATE CORRIDOR

A key parameter of the model is the central bank's interest rate corridor, as it determines the price of the outside options to interbank lending. We next analyze how changes in the corridor's width affect the interbank lending network and associated credit conditions.

Figure 10 shows how changes in the width of the corridor produce significant changes in the structure of the interbank lending network that are driven by changes in banks' monitoring and search efforts. Again, the uncertainty captured by the interquartile range largely captures the uncertainty about the precise latent distribution of liquidity shocks in the banking system. The most striking feature in Figure 10 is that an increase of roughly 100 percent in the width of the central bank's interest rate corridor (from 1 to 2 percentage points) produces over a three-fold increase in the mean network density (the average number of daily trades), going from a roughly 1 percent density to one that is over 3 percent. Furthermore, at a corridor width of 2 percentage points, the lower bound of the interquartile range across all network structures is larger than the upper bound on the interquartile range across network structures at a corridor width of 1 percentage point. This analysis shows that these effects on credit conditions are highly significant and that the interest rate corridor width plays an important role in the intensity of interbank activity.

Figure 10 illustrates a second important feature of the model—due to its nonlinear nature, the

³³Of course, other moments change as well in response to the shock. In particular, the distribution of monitoring and search efforts becomes more skewed.

multiplier's value is not constant over the range of corridor widths. In particular, Figure 10 shows that the multiplier's value decreases with the corridor width. Indeed, a 10 basis point increase of the bound has a much larger relative effect on the network density for lower corridor widths compared to larger ones. For instance, increasing the bound from 1.0 to 1.25 percentage points leads to a relative increase of about 45 percent in density, while an increase from 1.75 to 2.0 percentage points leads to a relative increase in density of about 28 percent. The presence of this multiplier, as well as its nonlinearity, are both explained by the role that monitoring and search efforts play in the interbank market. Similar to the Keynesian spending multiplier, the effects of a change in the width of the interest rate bounds can also be decomposed into (i) an immediate short-run effect, and (ii) a long-run effect that results from feedback loops between the effect of monitoring and search on loan outcomes, and expectations about credit conditions.

Consider a decrease in the width of the interest rate corridor. In response to this shock, the interbank market immediately shrinks, as a fraction of potential loans are no longer profitable given the tighter new bounds. The immediate mechanical effect is that part of the interbank market switches to lending and borrowing from the central bank, which now plays a more important role in credit markets. This immediate short-run effect, however, only constitutes a fraction of the total long-run multiplier effect. Indeed, given that the possibilities of interbank trading are now smaller, expected future profits are reduced, and the incentive to search for and monitor partners is diminished. This reduction in search and monitoring (depicted in Figure 10) will further reduce the mean density and mean traded-volumes in the interbank market. In turn, these reductions force banks to revise downward the expected profitability of monitoring and search efforts, further lowering these mean variables. This spiraling negative effect that defines the multiplier eventually will bring the market to a new operating level that may be orders of magnitude lower than the observed values prior to the imposition of the tighter interest rate bounds.

Similarly, an increase in the size of the interest rate corridor leads to wider participation in the interbank market, again fostered by banks' increased levels of monitoring. Moreover, from Figure 10 we find that with a wider interest rate corridor, both the mean spread of granted loans (relative to the center of the corridor) as well as the cross-sectional standard deviation increase, while the average (log) volume traded decreases. The changes in these market outcomes are driven by bank

pairs that did not trade under the narrower interest rate corridor but instead preferred to deposit funds at the central bank. Although interest rates remain high after the corridor is widened, trading becomes profitable for those bank pairs, driving up the average rate and the standard deviation of granted loans. Similarly, the trading network's reciprocity and stability decrease because with a wider corridor, trading becomes more attractive for those smaller banks that only occasionally seek to access the interbank market.

Hence, if the central bank wishes to get tighter control over the traded interbank rates by narrowing the interest rate corridor, it has to expect further adverse effects on interbank lending activity triggered by a reduction of counterparty search and monitoring. On the other hand, if the central bank wants to foster an active decentralized interbank lending market as a means to explore the benefits obtainable from peer monitoring, it is essential to consider policies that increase the rate differential between the interbank market and the standing facilities for depositing and lending funds. Only then is the interbank market profitable enough to encourage intense peer monitoring and search among banks. Regardless of whether the central bank wants to encourage or discourage using the interbank market, the multiplier effect should be taken into account when considering policy changes.

6 CONCLUSION

In this paper, we propose and develop a structural micro-founded network model for the unsecured OTC interbank market where banks can lend and borrow funds to smooth liquidity shocks or resort to using the central bank's standing facilities. Banks choose which counterparties to approach for bilateral Nash bargaining about interest rates and set their monitoring efforts to mitigate asymmetric information problems about counterparty risk. We estimate the structural model's parameters using network statistics for the Dutch unsecured overnight interbank lending market running from mid-February 2008 through April 2011.

Our model-based analysis shows that the prevailing bank-to-bank uncertainty and peer monitoring levels interact with counterparty search to generate an amplification mechanism that can replicate the key characteristics of interbank markets. First, banks form long-term lending relationships

that are associated with improved credit conditions. Second, the lending network exhibits a sparse core-periphery structure. Moreover, our dynamic analysis shows that shocks to credit-risk uncertainty can diminish lending activity for extended periods of time.

Based on our estimation results, we discuss the implications for monetary policy. In particular, we show that in order to foster trading activity in unsecured interbank markets and exploit the benefits from peer monitoring, an effective policy measure is to widen the bounds of the interest rate corridor. The full effects of a wider corridor are due to both a direct effect and a nonlinear indirect multiplier effect triggered by increased monitoring and search activity among banks.

For future research, we believe that our framework could be used to study several interesting extensions. First, in this paper we do not study the effects of liquidity hoarding and excess liquidity on market participation nor the bilateral bargaining problem and monitoring decisions.³⁴ Second, this paper leaves open the question of the optimal corridor size, which requires making assumptions about the central bank's preferences. Third, an interesting analysis would ask how the failure of an interbank relationship lender, an event that destroys private information, tightens credit conditions for its respective borrowers, thereby engendering the possibility that contagion may arise from the asset side.

³⁴For instance, in this paper we do not address the effects of the long-term refinancing operations as of the end of 2011.

REFERENCES

- Acemoglu, Daron, Asuman Ozdaglar, and Alireza Tahbaz-Salehi. 2015. “Systemic Risk and Stability in Financial Networks.” *American Economic Review* 105 (2):564–608.
- Acharya, Viral V., and Ouarda Merrouche. 2013. “Precautionary Hoarding of Liquidity and Interbank Markets: Evidence from the Subprime Crisis.” *Review of Finance* 17 (1):107–160.
- Affinito, Massimiliano. 2012. “Do Interbank Customer Relationships Exist? And How Did They Function Over the Crisis? Learning from Italy.” *Journal of Banking & Finance* 36 (12):3163–3184.
- Afonso, Gara, Anna Kovner, and Antoinette Schoar. 2011. “Stressed, Not Frozen: The Federal Funds Market in the Financial Crisis.” *Journal of Finance* 66 (4):1109–1139.
- Afonso, Gara, Anna Kovner, and Antoinette Schoar. 2013. “Trading Partners in the Interbank Lending Market.” Staff Reports No. 620. Federal Reserve Bank of New York.
- Afonso, Gara, and Ricardo Lagos. 2015. “Trade Dynamics in the Market for Federal Funds.” *Econometrica* 83 (1):263–313.
- Allen, Franklin, and Douglas Gale. 2000. “Financial Contagion.” *Journal of Political Economy* 108 (1):1–33.
- Arciero, Luca, Ronald Heijmans, Richard Heuver, Marco Massarenti, Cristina Picillo, and Francesco Vacirca. 2013. “How to Measure the Unsecured Money Market? The Eurosystem’s Implementation and Validation Using TARGET2 Data.” Working Paper No. 369. Amsterdam: De Nederlandsche Bank.
- Ashcraft, Adam B., and Darrell Duffie. 2007. “Systemic Illiquidity in the Federal Funds Market.” *The American Economic Review* 97 (2):221–225.
- Babus, Ana. 2013. “Endogenous Intermediation in Over-the-Counter Markets.” Unpublished working paper.
- Babus, Ana, and Péter Kondor. 2013. “Trading and Information Diffusion in OTC Markets.” Discussion Paper No. 9271. London: Center for Economic Policy Research.

- Bech, Morten L., and Enghin Atalay. 2010. “The Topology of the Federal Funds Market.” *Physica A: Statistical Mechanics and its Applications* 389 (22):5223–5246.
- Bech, Morten L., and Elizabeth Klee. 2011. “The Mechanics of a Graceful Exit: Interest on Reserves and Segmentation in the Federal Funds Market.” *Journal of Monetary Economics* 58 (5):415–431.
- Bech, Morten L., and Cyril Monnet. 2013. “The Impact of Unconventional Monetary Policy on the Overnight Interbank Market.” In *Liquidity and Funding Markets*, ed. Alexandra Heath, Matthew Lilley, and Mark Manning, RBA Annual Conference Volume. Sydney: Reserve Bank of Australia.
- Becher, Christopher, Stephen Millard, and Kimmo Soramäki. 2008. “The Network Topology of CHAPS Sterling.” Working Paper No. 355. London: Bank of England.
- Berentsen, Aleksander, and Cyril Monnet. 2008. “Monetary Policy in a Channel System.” *Journal of Monetary Economics* 55 (6):1067–1080.
- Bindseil, Ulrich, and Juliusz Jabłęcki. 2011. “The Optimal Width of the Central Bank Standing Facilities Corridor and Banks’ Day-to-Day Liquidity Management.” Working Paper Series No. 1350. Frankfurt: European Central Bank.
- Boss, Michael, Helmut Elsinger, Martin Summer, and Stefan Thurner. 2004. “Network Topology of the Interbank Market.” *Quantitative Finance* 4 (6):677–684.
- Bougerol, Philippe. 1993. “Kalman Filtering with Random Coefficients and Contractions.” *SIAM Journal on Control and Optimization* 31 (4):942–959.
- Broecker, Thorsten. 1990. “Credit-Worthiness Tests and Interbank Competition.” *Econometrica* 58 (2):429–452.
- Bräuning, Falk, and Falko Fecht. 2012. “Relationship Lending in the Interbank Market and the Price of Liquidity.” Discussion Papers No. 22/2012. Frankfurt: Deutsche Bundesbank.
- Chow, Gregory C. 1989. “Rational versus Adaptive Expectations in Present Value Models.” *Review of Economics and Statistics* 71 (3):376–384.

- Chow, Gregory C. 2011. “Usefulness of Adaptive and Rational Expectations in Economics.” Working Paper No. 1334. Department of Economics, Center for Economic Policy Studies. Princeton, NJ: Princeton University.
- Cocco, João F., Francisco J. Gomes, and Nuno C. Martins. 2009. “Lending Relationships in the Interbank Market.” *Journal of Financial Intermediation* 18 (1):24–48.
- Cœuré, Benoît. 2013. “Exit Strategies: Time to Think About Them.” Speech at the 15th Geneva Conference on the World Economy, <http://www.ecb.europa.eu/press/key/date/2013/html/sp130503.en.html>, Accessed on August 22, 2014.
- Craig, Ben, and Goetz von Peter. 2014. “Interbank Tiering and Money Center Banks.” *Journal of Financial Intermediation* 23 (3):322–347.
- de Frutos, Juan Calos, Carlos Garcia de Andoain, Florian Heider, and Patrick Papsdorf. 2014. “Stressed Interbank Markets: Evidence from the European Financial and Sovereign Debt Crisis.” Unpublished paper.
- DeJong, David N., and Chetan Dave. 2006. *Structural Macroeconometrics*. Princeton, NJ: Princeton University Press.
- Diamond, Douglas W., and Philip H. Dybvig. 1983. “Bank Runs, Deposit Insurance, and Liquidity.” *Journal of Political Economy* 91 (3):401–419.
- Duffie, Darrell, Nicolae Garleanu, and Lasse Heje Pedersen. 2005. “Over-the-Counter Markets.” *Econometrica* 73 (6):1815–1847.
- Evans, George W., and Seppo Honkapohja. 2001. *Learning and Expectations in Macroeconomics*. Princeton, NJ: Princeton University Press.
- Fagiolo, Giorgio. 2007. “Clustering in Complex Directed Networks.” *Physics Review E* 76:026107.
- Farboodi, Maryam. 2014. “Intermediation and Voluntary Exposure to Counterparty Risk.” Unpublished working paper.
- Fecht, Falko, Kjell G. Nyborg, and Jörg Rocholl. 2011. “The Price of Liquidity: The Effects of Market Conditions and Bank Characteristics.” *Journal of Financial Economics* 102 (2):344–362.

- Freixas, Xavier, and Cornelia Holthausen. 2005. "Interbank Market Integration under Asymmetric Information." *Review of Financial Studies* 18 (2):459–490.
- Freixas, Xavier, and José Jorge. 2008. "The Role of Interbank Markets in Monetary Policy: A Model with Rationing." *Journal of Money, Credit and Banking* 40 (6):1151–1176.
- Furfine, Craig H. 1999. "The Microstructure of the Federal Funds Market." *Financial Markets, Institutions & Instruments* 8 (5):24–44.
- Furfine, Craig H. 2001. "Banks as Monitors of Other Banks: Evidence from the Overnight Federal Funds Market." *Journal of Business* 74 (1):33–57.
- Gabrieli, Silvia, and Co-Pierre Georg. 2014. "A Network View on Money Market Freezes." Mimeo.
- Gai, Prasanna, Andrew Haldane, and Sujit Kapadia. 2011. "Complexity, Concentration and Contagion." *Journal of Monetary Economics* 58 (5):453–470.
- Gale, Douglas M., and Shachar Kariv. 2007. "Financial Networks." *American Economic Review* 97 (2):99–103.
- Georg, Co-Pierre. 2013. "The Effect of the Interbank Network Structure on Contagion and Financial Stability." *Journal of Banking & Finance* 77 (7):2216–2228.
- Gofman, Michael. 2014. "Efficiency and Stability of a Financial Architecture with Too-Interconnected-to-Fail Institutions." Unpublished working paper.
- Gourieroux, Christian, Alain Monfort, and Eric Renault. 1993. "Indirect Inference." *Journal of Applied Econometrics* 8 (S):S85–118.
- Heer, Burkhard, and Alfred Maußner. 2005. *Dynamic General Equilibrium Modelling*. Berlin: Springer.
- Heider, Florian, Marie Hoerova, and Cornelia Holthausen. 2015. "Liquidity Hoarding and Interbank Market Spreads: The Role of Counterparty Risk." *Journal of Financial Economics* 118 (2):336–454.
- Heijmans, Ronald, Richard Heuver, Clement Levallois, and Iman van Lelyveld. 2014. "Dynamic Visualization of Large Transaction Networks: the Daily Dutch Overnight Money Market." Working Paper Series No. 418. Amsterdam: De Nederlandsche Bank.

- Heijmans, Ronald, Richard Heuver, and Daniëlle Walraven. 2011. “Monitoring the Unsecured Interbank Money Market Using TARGET2 Data.” Working Paper Series No. 276. Amsterdam: De Nederlandsche Bank.
- in ’t Veld, Daan, Marco van der Leij, and Cars Hommes. 2014. “The Formation of a Core Periphery Structure in Heterogeneous Financial Networks.” Tinbergen Institute Discussion Paper No. 14-098/II. Amsterdam: Tinbergen Institute.
- Iori, Giulia, Giulia De Masi, Ovidiu Vasile Precup, Giampaolo Gabbi, and Guido Caldarelli. 2008. “A Network Analysis of the Italian Overnight Money Market.” *Journal of Economic Dynamics and Control* 32 (1):259–278.
- Jackson, Matthew O. 2008. *Social and Economic Networks*. Princeton, NJ: Princeton University Press.
- Judd, Kenneth L. 1998. *Numerical Methods in Economics*. Cambridge, MA: The MIT Press.
- Kahn, George A. 2010. “Monetary Policy Under a Corridor Operating Framework.” *Federal Reserve Bank of Kansas City Economic Review* (Q IV):5–34.
- Lux, Thomas, and Daniel Fricke. 2012. “Core-Periphery Structure in the Overnight Money Market: Evidence from the e-MID Trading Platform.” Kiel Working Paper No. 1759. Kiel: Kiel Institute for the World Economy.
- May, Robert M., Simon A. Levin, and George Sugihara. 2008. “Complex Systems: Ecology for Bankers.” *Nature* 451 (7181):893–895.
- Poole, William. 1968. “Commercial Bank Reserve Management In A Stochastic Model: Implications For Monetary Policy.” *Journal of Finance* 23 (5):769–791.
- Rochet, Jean-Charles, and Jean Tirole. 1996. “Interbank Lending and Systemic Risk.” *Journal of Money, Credit and Banking* 28 (4):733–762.
- Ruge-Murcia, Francisco J. 2007. “Methods to Estimate Dynamic Stochastic General Equilibrium Models.” *Journal of Economic Dynamics and Control* 31 (8):2599–2636.

- Soramäki, Kimmo, Morten L. Bech, Jeffrey Arnold, Robert J. Glass, and Walter E. Beyeler. 2007. “The Topology of Interbank Payment Flows.” *Physica A: Statistical Mechanics and its Applications* 379 (1):317–333.
- van Lelyveld, Iman, and Daan in ’t Veld. 2014. “Finding the Core: Network Structure in Interbank Markets.” *Journal of Banking & Finance* 49 (December):27–40.
- Vuilleme, Guillaume, and Régis Breton. 2014. “Endogenous Derivative Networks.” Working Paper No. 483. Paris: Banque de France.
- White, Halbert. 2001. *Asymptotic Theory for Econometricians*. Revised Edition. Orlando, FL: Academic Press.
- Whitesell, William. 2006. “Interest Rate Corridors and Reserves.” *Journal of Monetary Economics* 53 (6):1177–1195.

FIGURES

Figure 1: Timeline Illustrating the Sequence of Events in Period t

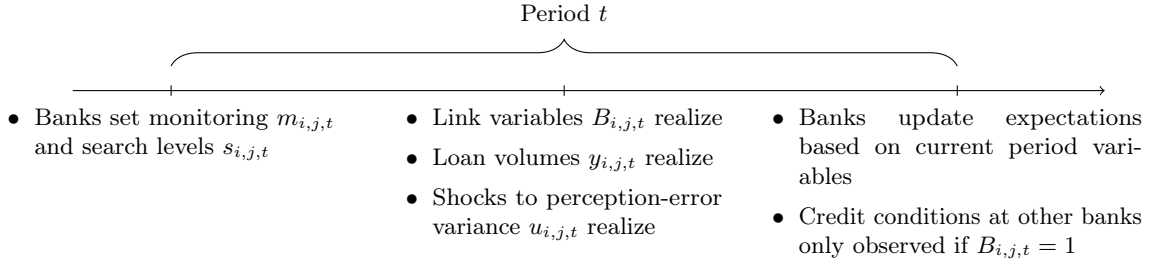
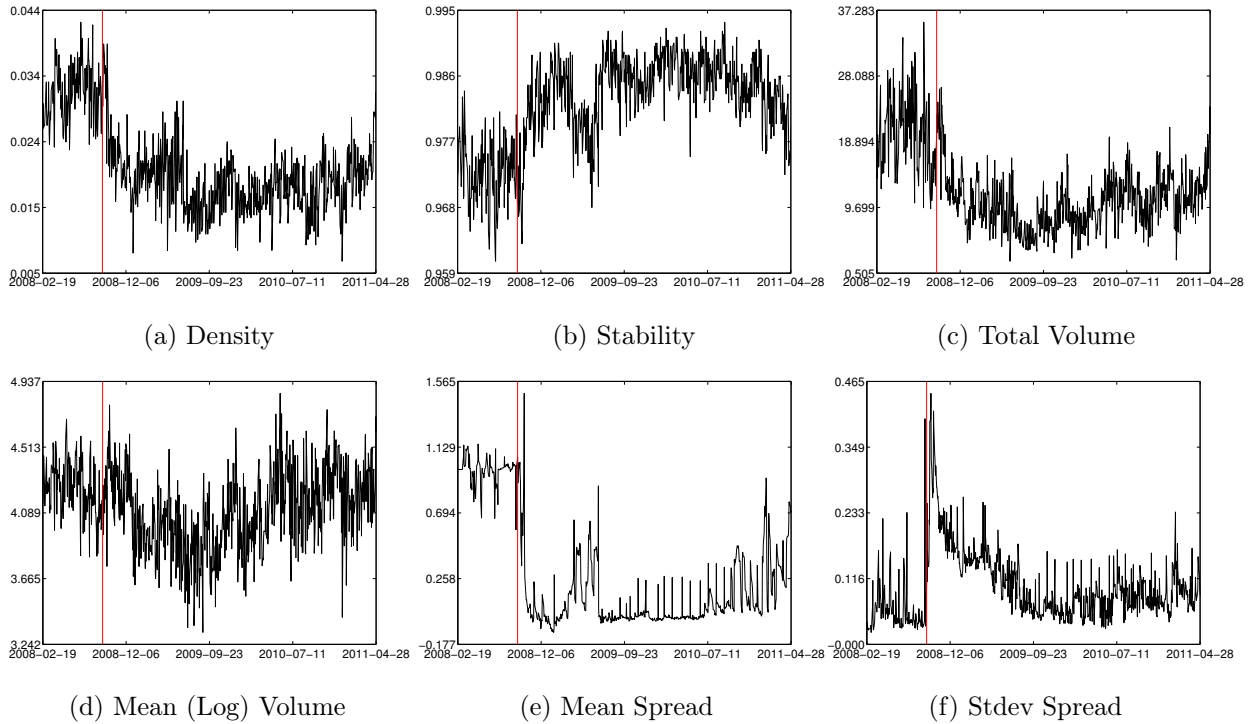


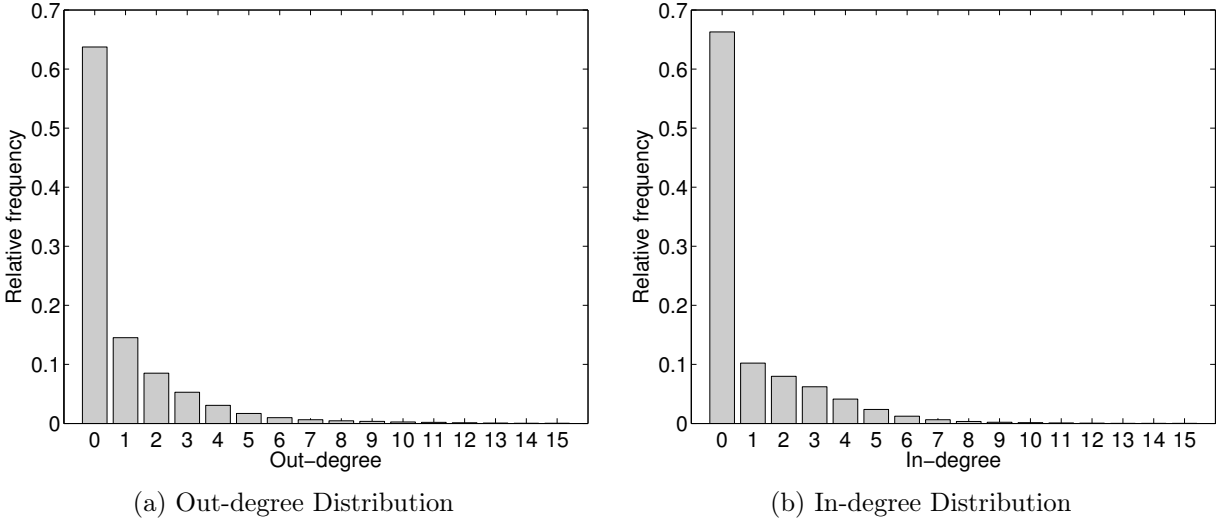
Figure 2: Daily Network Time Series Plots: February 18, 2008, to April 28, 2011



Notes: Time series plots of daily network density, stability, total traded volume (in EUR billions), and mean loan volume (in log EUR millions), mean spread (to deposit rate), and standard deviation of granted loans from February 18, 2008, to April 28, 2011. Vertical red line corresponds to Lehman's failure on September 15, 2008.

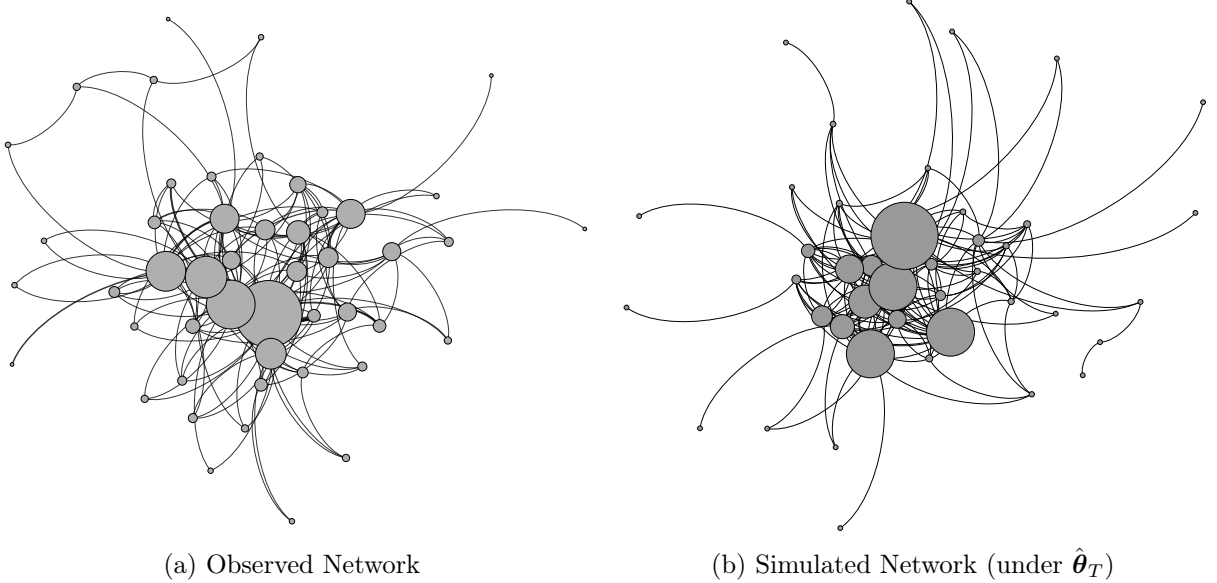
Source: Authors' calculations.

Figure 3: Degree Distribution Under the Estimated Parameter Vector $\hat{\theta}_T$



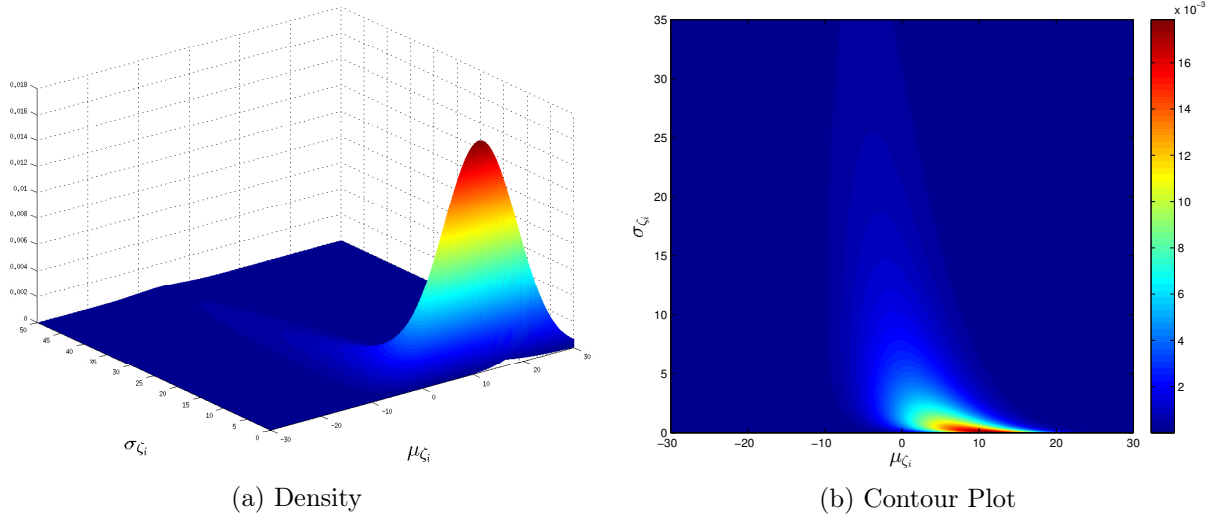
Notes: Marginal in- and out-degree distributions computed based on 5,000 simulated network paths of size $T = 25$ under the estimated parameter vector $\hat{\theta}_T$.
Source: Authors' calculations.

Figure 4: Interbank Network Market Structure for One Trading Week



Notes: Nodes are scaled according to total trading volume. The observed network corresponds to first week in April 2008; simulated network under estimated parameter $\hat{\theta}_T$ is randomly picked realization. Isolated nodes are not shown.
Source: Authors' calculations.

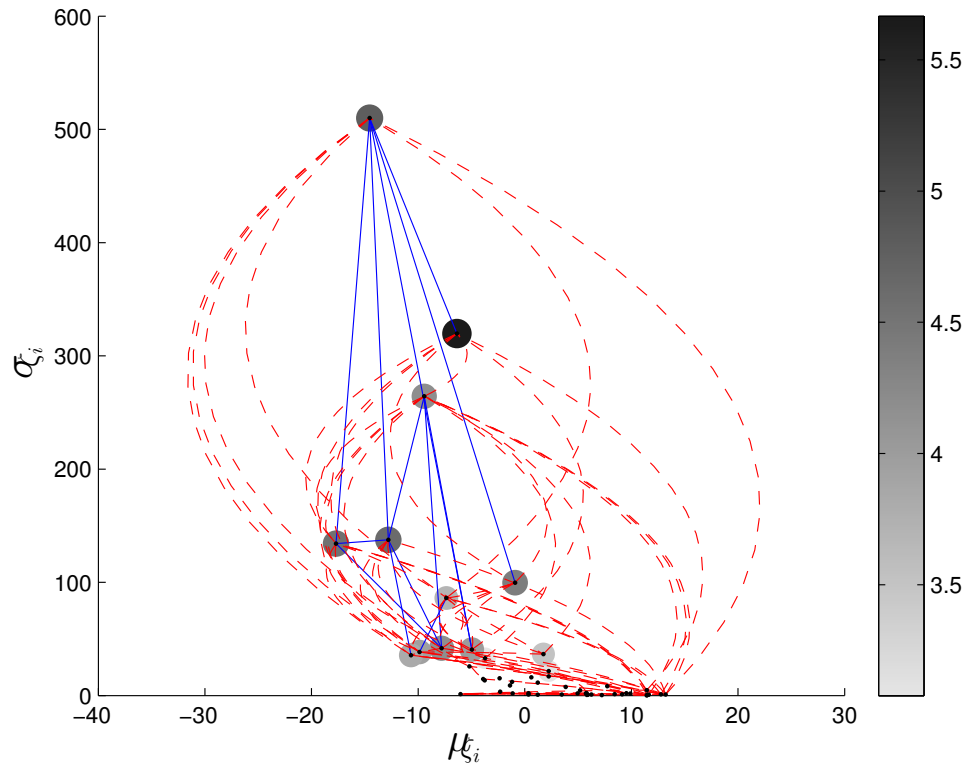
Figure 5: Liquidity Shock Distribution under Estimated Model Parameter



Notes: Joint distribution of mean (μ_{ζ_i}) and standard deviation (σ_{ζ_i}) of banks' liquidity shock distributions and contour plots as implied by the estimated model parameters.

Source: Authors' calculations.

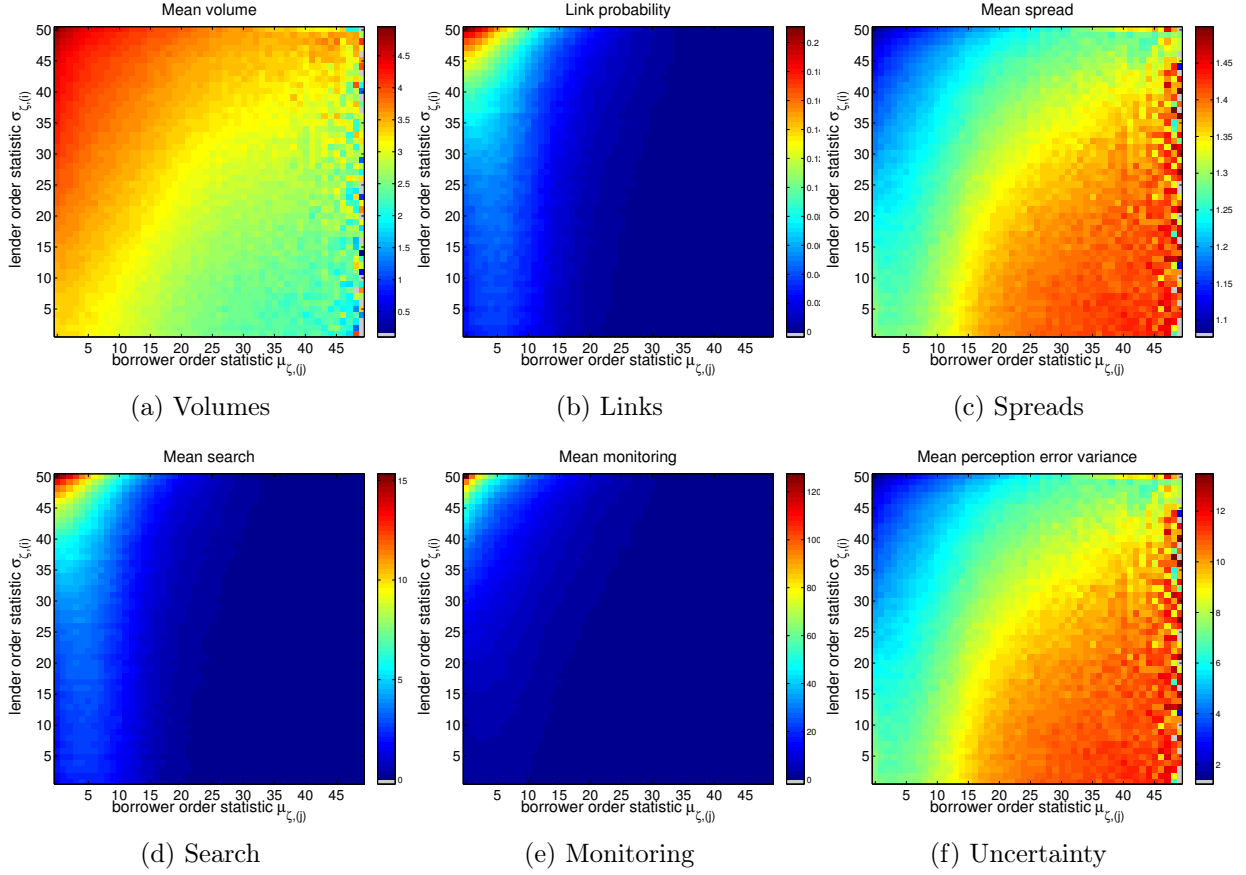
Figure 6: Simulated Interbank Activity for One Trading Week



Notes: A bank's position in the μ_ζ - σ_ζ plane is given by the mean and standard deviation parameters $(\mu_{\zeta i}, \sigma_{\zeta i})$. Node shading relates to average log loan volume per bank (right scale). For each node, incoming links are shown as dashed red lines coming from the right; outgoing links leave nodes from the left (counterclockwise). Solid blue lines represent reciprocal links.

Source: Authors' calculations.

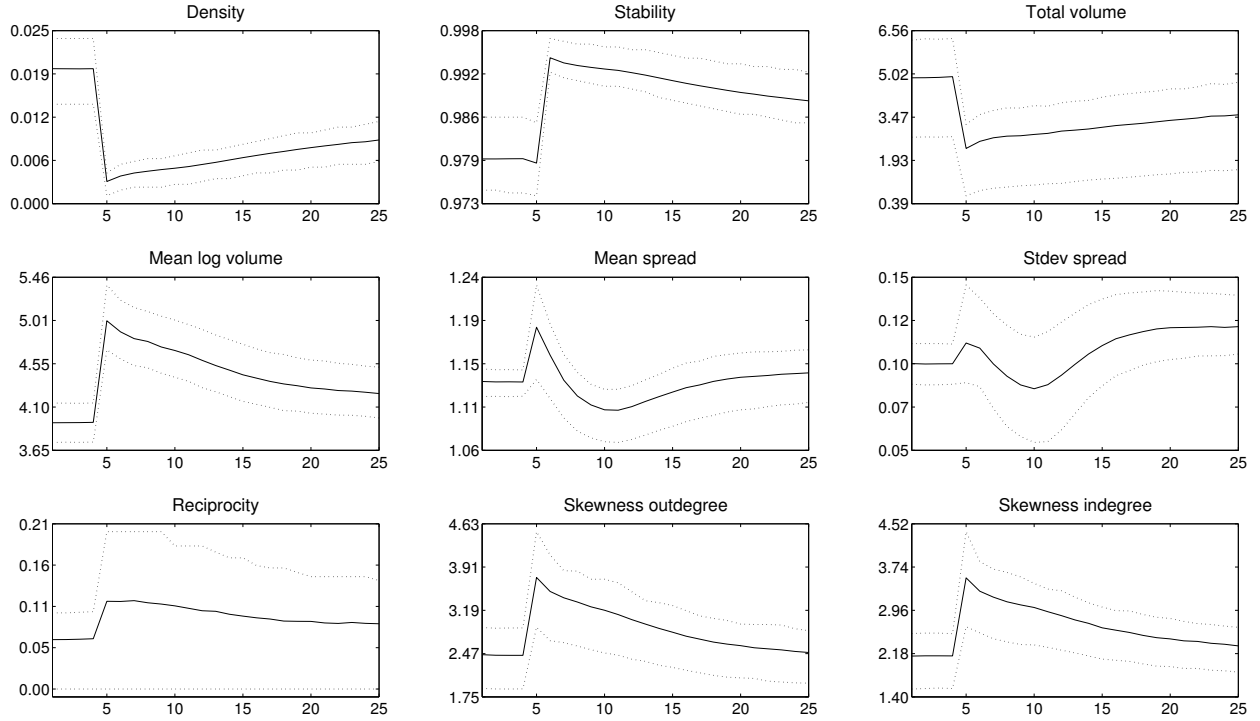
Figure 7: Bank Heterogeneity and Trading Relationships



Notes: The order statistics for the lender variance parameters $\sigma_{\zeta(i)}$ are depicted on the vertical axis, while the order statistics for the borrower mean parameters $\mu_{\zeta(i)}$ are depicted on the horizontal axis, that is, lender banks are ordered by variance parameter σ_{ζ^i} such that $\sigma_{\zeta^{50}} > \sigma_{\zeta^{49}} > \dots > \sigma_{\zeta^1}$, and borrower banks are ordered by mean parameter such that $\mu_{\zeta^{50}} > \mu_{\zeta^{49}} > \dots > \mu_{\zeta^1}$. The results are based on 10,000 MC repetitions, each of length $T = 100$.

Source: Authors' calculations.

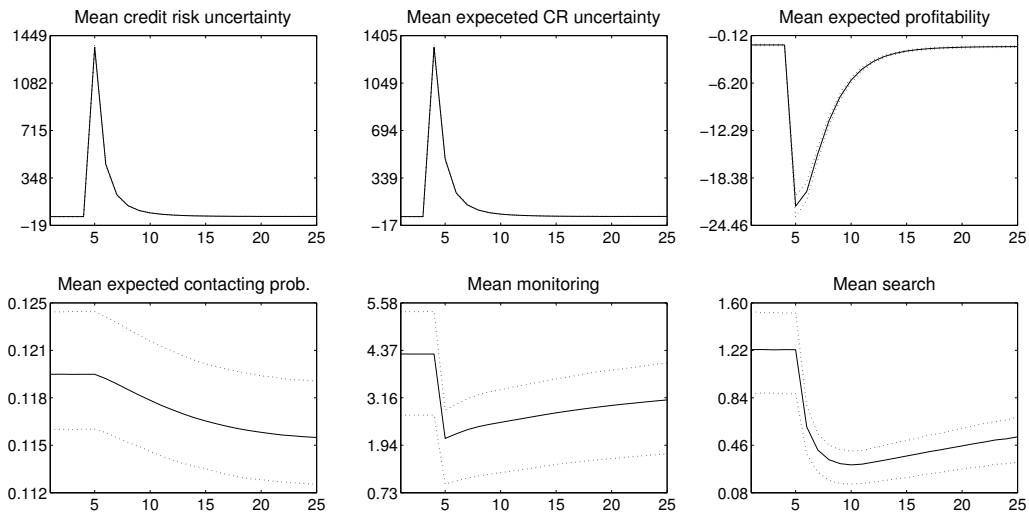
Figure 8: Impulse Responses to a Shock in Credit-Risk Uncertainty



Notes: Simulated impulse responses to a common 10 standard deviations shock in credit-risk uncertainty in period four. Results are based on 5,000 MC repetitions. The solid line is the mean impulse response, and the dotted lines refer to the interquartile range across all network structures. Total volume is in billions, and mean volume is the mean log volume (in millions) of granted loans.

Source: Authors' calculations.

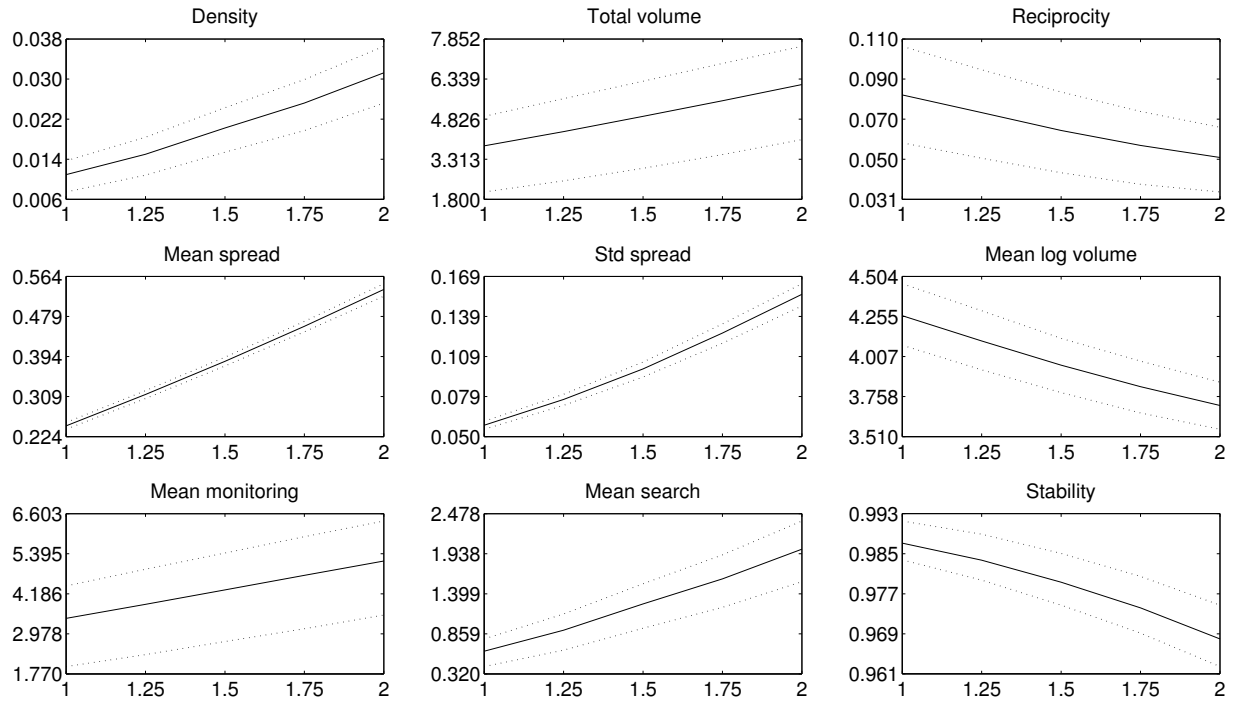
Figure 9: Impulse Responses to a Shock in Credit-Risk Uncertainty



Notes: Simulated impulse responses to a common 10 standard deviation shock in credit-risk uncertainty in $t = 4$. Results are based on 5,000 MC repetitions. The solid line is the mean impulse response, and the dotted lines refer to the interquartile range across all network structures. Expectations are in deviations from steady-state values. Monitoring and search expenditures are in thousands of euros.

Source: Authors' calculations.

Figure 10: Changes in the Central Bank's Interest Rate Corridor Width



Notes: Simulated mean and interquartile range of key network statistics and mean monitoring and mean search per bank over alternative interest corridor width. Total volume is in billion euros. The Monte Carlo results are based on 5,000 networks each with $T = 25$.

Source: Authors' calculations.

TABLES

Table 1: Descriptive Statistics

Statistic	Mean	Std	Autocorr
Density	0.0212	0.0068	0.8174
Reciprocity	0.0819	0.0495	0.2573
Stability	0.9818	0.0065	0.8309
Mean Out-/In-degree	1.0380	0.3323	0.8174
Mean Clustering	0.0308	0.0225	0.4149
$\text{Corr}(r_{i,j,t}, l_{i,j,t-1}^{rw})$	-0.0716	0.1573	0.4066
$\text{Corr}(l_{i,j,t}, l_{i,j,t-1}^{rw})$	0.6439	0.0755	0.4287
Mean Log Volume	4.1173	0.2818	0.4926
Mean Spread	0.2860	0.3741	0.9655

Notes: The table reports moment statistics for different sequences of network statistics and cross-sectional correlations that characterize the sequence of observed Dutch unsecured interbank lending networks. The statistics are computed on a sample of daily frequency from February 18, 2008, to April 28, 2011.

Table 2: Estimated Structural Parameter Values

Structural Parameter		Calibrated	Estimated		Estimated	
		Without Monitoring	Without Monitoring	Without Monitoring	With Monitoring	With Monitoring
		θ^r	$\hat{\theta}_T^r$	ste($\hat{\theta}_T^r$)	$\hat{\theta}_T$	ste($\hat{\theta}_T$)
Added Information	α_ϕ	-1.5000	-1.5000	-	-1.5000	-
	$\beta_{\phi,1}$	0.0000	0.0000	-	9.6631	0.0006
	$\beta_{\phi,2}$	0.0001	0.1386	0.0069	0.0001	0.0445
Perception Error variance	α_σ	1.2890	1.2449	0.0151	1.2890	0.0028
	β_σ	-2.0000	-2.0000	-	-2.0000	-
	γ_σ	0.6648	0.6351	0.0063	0.6648	0.0183
	δ_σ	0.3383	1.7214	0.0069	0.3383	0.0451
	α_λ	0.0001	0.0208	0.0566	0.0001	0.1159
Search Technology	β_λ	72.833	102.82	0.0009	72.833	0.0006
	μ_μ	0.0000	0.0000	-	0.0000	-
Liquidity Shocks	σ_μ^*	1.9903	3.6563	0.0024	1.9903	0.0228
	μ_σ	1.9492	0.6120	0.0033	1.9492	0.0218
	σ_σ	1.9810	4.5002	0.0051	1.9810	0.0213
	ρ_ζ	-0.7826	-0.0170	0.0064	-0.7826	0.0423
	λ^y	0.8472	0.8809	0.0226	0.8472	0.0443
Expectations	λ^B	-	-	-	0.9278	0.0470
	λ^r	0.4008	0.0180	0.0271	0.4008	0.0466
	$\lambda^{\tilde{\sigma}}$	-	-	-	0.0318	0.0414
	θ	0.6897	0.0054	0.0226	0.6896	0.0441
Interest Rate Corridor Width	r	1.5000	1.5000	-	1.5000	-
Default Threshold	ϵ	3.0000	3.0000	-	3.0000	-
Financial Distress Std.	σ	0.1000	0.1000	-	0.1000	-
Discount Rate	r^d	1.7500	1.7500	-	1.7500	-

Notes: This table reports the estimated structural parameters of the unrestricted model $\hat{\theta}_T$ and corresponding standard errors. For comparison, this table also reports the estimated parameter $\hat{\theta}_T^r$ of the restricted model without monitoring ($\beta_{\phi,1}=0$), as well as the calibrated parameter θ_a that equals $\hat{\theta}_T$ but sets the effect of monitoring to zero ($\beta_{\phi,1}=0$). For calibrated parameters, no standard errors are reported. The indirect inference estimator is based on $S = 24$ simulated network paths, each of length 3,000 periods, and the auxiliary statistics reported in Table 4. The parameters λ^B and $\lambda^{\tilde{\sigma}}$ are not part of the restricted model without monitoring. Note also that $\sigma_\mu^* = \log(\sigma_\mu)$.

Table 3: Coefficients of the Linear Policy Rule for Optimal Monitoring as Implied by $\hat{\theta}_T$

Variable	$\tilde{\sigma}_{i,j,t}$	$\mathbb{E}_t \tilde{\sigma}_{i,j,t+1}$	$\mathbb{E}_t B_{i,j,t+1}$	$\mathbb{E}_t y_{i,j,t+1}$
Coefficient	0.0024	-0.0043	0.0348	0.0019

Table 4: Auxiliary Network Statistics

Auxiliary Statistic	Simulated Values			Observed Values	
	Calibrated Without Monitoring	Estimated Without Monitoring	Estimated With Monitoring	$\hat{\beta}_T$	$\text{ste}(\hat{\beta}_T)$
	$\tilde{\beta}_{TS}(\theta^r)$	$\tilde{\beta}_{TS}(\hat{\theta}_T^r)$	$\tilde{\beta}_{TS}(\hat{\theta}_T)$		
Density (Mean)	0.1121	0.0201	0.0193	0.0212	0.0026
Reciprocity (Mean)	0.0453	0.0005	0.0627	0.0819	0.0029
Stability (Mean)	0.8247	0.9837	0.9795	0.9818	0.0025
Avg Clustering (Mean)	0.1097	0.0042	0.0347	0.0308	0.0027
Avg Degree (Mean)	5.4948	0.9870	0.9441	1.0380	0.1291
Std Outdegree (Mean)	3.2901	1.3501	1.6547	1.8406	0.0918
Skew Out-degree (Mean)	0.4512	1.3604	2.3649	2.8821	0.3537
Std In-degree (Mean)	4.7450	1.3833	1.6950	1.6001	0.0995
Skew In-degree (Mean)	0.3300	1.3971	2.2801	2.4030	0.3143
Corr($r_{i,j,t}, l_{i,j,t-1}^{rw}$) (Mean)	0.0000	-0.1578	-0.1231	-0.0716	0.0113
Corr($l_{i,j,t}, l_{i,j,t-1}^{rw}$) (Mean)	0.2345	0.4259	0.6001	0.6439	0.0107
Avg Log Volume (Mean)	2.8298	4.1064	3.9422	4.1173	0.0516
Std Log Volume (Mean)	1.0547	1.0196	1.0865	1.6896	0.0200
Skew Log Volume (Mean)	-0.1187	-0.2958	-0.1357	-0.3563	0.0317
Avg Spread (Mean)	1.0348	0.4604	1.1353	0.2860	0.1331
Std Spread (Mean)	0.0000	0.4046	0.1004	0.1066	0.0142
Skew Spread (Mean)	0.0251	0.8658	1.6010	0.6978	0.5295
Corr(Density,Stability)	-0.4688	-0.4253	-0.3837	-0.7981	0.0275
Corr(Density,Avg Spread)	0.0296	-0.0003	0.0896	0.7960	0.0229
Autocorr(Density)	0.0034	0.5697	0.2455	0.8174	0.0243
Autocorr(Avg Volume)	0.0014	0.3875	0.0760	0.4926	0.0555
Autocorr(Avg Spread)	0.9991	0.1624	0.2425	0.9655	0.0031
Objective Function Value	227.3328	6.5852	4.2407		
Euclidean Norm $\ \hat{\beta}_T - \tilde{\beta}_{TS}\ $	6.8563	2.4022	2.0035		
Sup Norm $\ \hat{\beta}_T - \tilde{\beta}_{TS}\ _\infty$	4.4568	1.5217	0.9032		

Notes: The table reports the values of the observed auxiliary statistics $\hat{\beta}_T$ used in the indirect inference estimation along with the HAC robust standard errors, as well as the simulated average of the auxiliary statistics for different model parameterizations: (i) for the estimated parameter vector of the unrestricted model $\hat{\theta}_T$; (ii) for the calibrated vector θ^r that equals $\hat{\theta}_T$ but sets the effect of monitoring to zero ($\beta_{\phi,1}=0$); and (iii) for the estimated parameter vector of the restricted model without monitoring $\hat{\theta}_T^r$ (with the restriction $\beta_{\phi,1}=0$). The observed statistics are computed on a sample of daily frequency from February 18, 2008, to April 28, 2011, of size $T = 810$. The objective function is a quadratic form with diagonal weight matrix using $S = 24$ simulated network paths, each of length 3,000 periods (see Equation 4.1). For the different structural parameter vectors, see Table 2. Density is not included in the vector of auxiliary statistics as the density is proportional to average degree.

APPENDIX A MODEL SOLUTION

The variable $l_{i,j,t} = B_{i,j,t} \cdot \mathbb{I}(r_{i,j,t} \leq r) \cdot \mathbb{I}(y_{i,j,t} > 0)$ introduces a discontinuity that prevents us from obtaining analytic optimality conditions of the original optimization problem stated in Equation 7. Although numerical solutions are theoretically possible, these would make simulation and estimation prohibitively time-consuming given the high dimensional problem.

We therefore consider an approximate smooth problem where we replace the original problem's step functions ($\mathbb{I}(r_{i,j,t} \leq r)$) by a continuously differentiable logistic function $I(r_{i,j,t}) = \frac{1}{1 + \exp(-\beta_I(r - r_{i,j,t}))} =: I_{i,j,t}$. Note that for a growing scale parameter, the logistic transformation approximates the step function arbitrarily well. Without changing the notation, we redefine $l_{i,j,t} = B_{i,j,t} I_{i,j,t}$, where we dropped the factor $\mathbb{I}(y_{i,j,t} > 0)$ without changing the optimization problem, as by the construction of $y_{i,j,t}$, funds are exchanged only if i has a surplus and j a deficit.

We can solve this approximate optimization problem using the well-understood calculus of variations, the most widely applied method to solve constrained dynamic stochastic optimization problems in structural economics (see, for example, Judd 1998 and DeJong and Dave 2006). Substituting out all definitions in the objective function, except for the law of motion for $\tilde{\sigma}_{i,j,t}^2$, we can write the Lagrange function of the optimization problem with multiplier $\mu_{i,j,t}$ given by

$$\mathcal{L} = \mathbb{E}_t \sum_{s=t}^{\infty} \left(\frac{1}{1 + r^d} \right)^{s-t} \sum_{j=1}^N \pi_{i,j,t}(m_{i,j,t}, s_{j,i,t}, \tilde{\sigma}_{i,j,t}^2) + \mu_{i,j,t} (\xi(m_{i,j,t}, \tilde{\sigma}_{i,j,t}^2) - \tilde{\sigma}_{i,j,t+1}^2),$$

where we make explicit the arguments that can be influenced by bank i 's decision. The Euler equations that establish the first-order-conditions to the infinite-horizon nonlinear dynamic stochastic optimization problem can then be obtained by optimizing the Lagrange function with respect to the control variables and the dynamic constraints (see, for example, Heer and Maußner 2005).

Under usual regularity conditions, the integration and differentiation steps can be interchanged,

and we obtain

$$\begin{aligned}
\frac{\partial \mathcal{L}}{\partial m_{i,j,t}} = 0 &\Leftrightarrow \mathbb{E}_t \left[\frac{\partial \pi_{i,j,t}}{\partial m_{i,j,t}} + \mu_{i,j,t} \frac{\partial \xi_{i,j,t}}{\partial m_{i,j,t}} \right] = 0 \\
\frac{\partial \mathcal{L}}{\partial \tilde{\sigma}_{i,j,t+1}^2} = 0 &\Leftrightarrow \mathbb{E}_t \left[-\mu_{i,j,t} + \frac{1}{1+r^d} \left(\frac{\partial \pi_{i,j,t+1}}{\partial \tilde{\sigma}_{i,j,t+1}^2} + \mu_{i,j,t+1} \frac{\partial \xi_{i,j,t+1}}{\partial \tilde{\sigma}_{i,j,t+1}^2} \right) \right] = 0 \\
\frac{\partial \mathcal{L}}{\partial s_{i,j,t}} = 0 &\Leftrightarrow \mathbb{E}_t \left[\frac{\partial \pi_{i,j,t}}{\partial s_{i,j,t}} \right] = 0 \\
\frac{\partial \mathcal{L}}{\partial \mu_{i,j,t}} = 0 &\Leftrightarrow \mathbb{E}_t \left[\tilde{\sigma}_{i,j,t+1}^2 - \xi(\phi_{i,j,t}, \tilde{\sigma}_{i,j,t}^2) \right] = 0,
\end{aligned}$$

for all counterparties $j \neq i$ and all t . Substituting out the Lagrange multipliers and taking fixed values at time t out of the expectation gives the Euler equation for the optimal monitoring path that equates marginal cost and discounted expected future marginal benefits of monitoring,

$$\frac{1}{1+r^d} \frac{\partial \xi_{i,j,t}}{\partial m_{i,j,t}} \mathbb{E}_t \left(\frac{\frac{\partial \xi_{i,j,t+1}}{\partial \tilde{\sigma}_{i,j,t+1}^2}}{\frac{\partial \xi_{i,j,t+1}}{\partial m_{i,j,t+1}}} + \frac{\partial \pi_{i,j,t+1}}{\partial \tilde{\sigma}_{i,j,t+1}^2} \right) = 1. \quad (13)$$

Unlike monitoring expenditures, search becomes effective in the same period it is exerted and does not directly alter future matching probabilities via a dynamic constraint. Thus, the first-order condition for the optimal search path is given by

$$\frac{\partial}{\partial s_{i,j,t}} \mathbb{E}_t \left[(r - r_{j,i,t}) y_{j,i,t} l_{j,i,t} \right] = 1, \quad (14)$$

leading to the usual condition that the expected marginal benefit equals the marginal cost in each period without any discounting. Since the first-order conditions hold for all $j \neq i$ and the marginal cost of monitoring and search is the same across all j , the conditions also imply that (discounted) expected marginal profits of monitoring and search must be the same across different banks j .

The transversality condition for the dynamic problem is obtained as the limit to the endpoint condition from the corresponding finite horizon problem and requires that

$$\lim_{T \rightarrow \infty} \mathbb{E}_t \left[\left(\frac{1}{1+r^d} \right)^{T-2} \frac{\partial \pi_{i,j,T-1}}{\partial m_{i,j,T-1}} - \left(\frac{1}{1+r^d} \right)^{T-1} \frac{\partial \pi_{i,j,T}}{\partial \tilde{\sigma}_{i,j,T}^2} \frac{\partial \xi_{i,j,T-1}}{\partial m_{i,j,T-1}} \right] = 0.$$

Thus, in the limit the expected marginal cost of investing in monitoring must be equal to the

expected marginal return.

Equations (13) and (14) constitute the first-order conditions to banks' approximate optimization problem. From the first-order condition for the optimal search expenditure in Equation (14) we get

$$\begin{aligned} & \frac{\partial}{\partial s_{i,j,t}} \mathbb{E}_t \left[(r - r_{j,i,t}) y_{j,i,t} l_{j,i,t} \right] = 1 \\ \Leftrightarrow & \frac{\partial}{\partial s_{i,j,t}} \mathbb{E}_t \left[(r - r_{j,i,t}) y_{j,i,t} I_{j,i,t} B_{j,i,t} \right] = 1 \\ \Leftrightarrow & \mathbb{E}_t \left[(r - r_{j,i,t}) y_{j,i,t} I_{j,i,t} \right] \frac{\beta_\lambda \exp(-\beta_\lambda (s_{i,j,t} - \alpha_\lambda))}{(1 + \exp(-\beta_\lambda (s_{i,j,t} - \alpha_\lambda)))^2} = 1 \end{aligned}$$

where the first step uses the definition of $l_{j,i,t}$, and the second step uses the independence of $B_{j,i,t}$. The above equation can be solved analytically for $s_{i,j,t}$ leading to Equation (10).

The first-order condition for monitoring in Equations (13) is

$$1 = \frac{1}{1 + r^d} \frac{\partial \xi_{i,j,t}}{\partial m_{i,j,t}} \mathbb{E}_t \left(\frac{\frac{\partial \xi_{i,j,t+1}}{\partial \tilde{\sigma}_{i,j,t+1}^2} - \frac{\partial \pi_{i,j,t+1}}{\partial \tilde{\sigma}_{i,j,t+1}^2}}{\frac{\partial \xi_{i,j,t+1}}{\partial m_{i,j,t+1}}} \right).$$

Using the product rule, we get $\frac{\partial \pi_{i,j,t}}{\partial \tilde{\sigma}_{i,j,t}^2} = \frac{\partial \bar{R}_{i,j,t}}{\partial \tilde{\sigma}_{i,j,t}^2} y_{i,j,t} l_{i,j,t} + \bar{R}_{i,j,t} y_{i,j,t} B_{i,j,t} \frac{\partial I_{i,j,t}}{\partial \tilde{\sigma}_{i,j,t}^2}$, which we can further unfold using the following partial derivatives

$$\begin{aligned} \frac{\partial \phi_{i,j,t}}{\partial m_{i,j,t}} &= \beta_\phi, & \frac{\partial P_{i,j,t}}{\partial \tilde{\sigma}_{i,j,t}^2} &= \frac{\epsilon^2}{(\sigma^2 + \tilde{\sigma}_{i,j,t}^2 + \epsilon^2)^2}, & \frac{\partial r_{i,j,t}}{\partial \tilde{\sigma}_{i,j,t}^2} &= 0.5/\epsilon^2 \\ \frac{\partial \xi_{i,j,t}}{\partial \phi_{i,j,t}} &= \exp(\alpha_\sigma + \gamma_\sigma \log \tilde{\sigma}_{i,j,t}^2 + \beta_\sigma \phi_{i,j,t} + \delta_\sigma u_{i,j,t}) \beta_\sigma, \\ \frac{\partial \xi_{i,j,t}}{\partial \tilde{\sigma}_{i,j,t}^2} &= \exp(\alpha_\sigma + \gamma_\sigma \log \tilde{\sigma}_{i,j,t}^2 + \beta_\sigma \phi_{i,j,t} + \delta_\sigma u_{i,j,t}) / \tilde{\sigma}_{i,j,t}^2, \\ \frac{\partial \bar{R}_{i,j,t}}{\partial \tilde{\sigma}_{i,j,t}^2} &= -\frac{\partial P_{i,j,t}}{\partial \tilde{\sigma}_{i,j,t}^2} + \frac{\partial 1 - P_{i,j,t}}{\partial \tilde{\sigma}_{i,j,t}^2} r_{i,j,t} + (1 - P_{i,j,t}) \frac{\partial r_{i,j,t}}{\partial \tilde{\sigma}_{i,j,t}^2} \\ \frac{\partial I_{i,j,t}}{\partial \tilde{\sigma}_{i,j,t}^2} &= \frac{\beta_I \exp(-\beta_I (r - r_{i,j,t}))}{1 + \exp(-\beta_I (r - r_{i,j,t}))} \left(-\frac{\partial r_{i,j,t}}{\partial \tilde{\sigma}_{i,j,t}^2} \right). \end{aligned}$$

Equation (13) is highly nonlinear and does not have an analytical solution. We therefore follow the standard practice to compute an approximate solution based on a Taylor expansion. To this end,

write the Euler equation more compactly as

$$\mathbb{E}_t f(m_{i,j,t}, \tilde{\sigma}_{i,j,t}^2, \tilde{\sigma}_{i,j,t+1}^2, B_{i,j,t+1}, y_{i,j,t+1}) = 0.$$

The local Taylor approximation of f requires an expansion point. The usual steady state (resulting from the absence of any shocks to the system) proves inappropriate in our setting, as steady state volumes would be zero and, as a consequence, the steady state corresponds to a critical point where all derivatives of f are zero. We therefore linearize the function f around the stable point $(\tilde{m}_{i,j}, \tilde{\sigma}_{i,j}^2, \tilde{\sigma}_{i,j}^2, \tilde{\lambda}_{i,j}, \tilde{y}_{i,j})$. This expansion point is obtained as the steady state of the system when $y_{i,j,t+1}$ is fixed at the expected loan volumes for two banks characterized by a liquidity shock distribution with mean parameter $\mathbb{E}(\mu_{\zeta^i}) = \mu_\mu$ and variance parameter $\mathbb{E}(\sigma_{\zeta^i}^2) = \exp(\mu_\sigma + \sigma_\sigma^2/2)$ (two ‘‘average’’ banks).³⁵ As a result the expansion point is the same for each bank pair (i, j) .³⁶

In the following expansion we write $h_x := \frac{\partial h(x,y)}{\partial x}$ and use $\hat{x} := x - \tilde{x}$ to denote a deviation from the expansion point. Applying the first-order Taylor expansion gives

$$f \approx \tilde{f} + f_{m_{i,j,t}} \hat{m}_{i,j,t} + f_{\tilde{\sigma}_{i,j,t}^2} \hat{\tilde{\sigma}}_{i,j,t}^2 + f_{\tilde{\sigma}_{i,j,t+1}^2} \hat{\tilde{\sigma}}_{i,j,t+1}^2 + f_{B_{i,j,t+1}} \hat{B}_{i,j,t+1} + f_{y_{i,j,t+1}} \hat{y}_{i,j,t+1}$$

where $\tilde{f} := f(\tilde{m}_{i,j}, \tilde{\sigma}_{i,j}^2, \tilde{\sigma}_{i,j}^2, \tilde{\lambda}_{i,j}, \tilde{y}_{i,j})$ and all derivatives are evaluated at the expansion point. Note that $\tilde{f} = 0$ by construction.

We then obtain the approximate Euler equation for monitoring as

$$\mathbb{E}_t [f_{m_{i,j,t}} \hat{m}_{i,j,t} + f_{\tilde{\sigma}_{i,j,t}^2} \hat{\tilde{\sigma}}_{i,j,t}^2 + f_{\tilde{\sigma}_{i,j,t+1}^2} \hat{\tilde{\sigma}}_{i,j,t+1}^2 + f_{B_{i,j,t+1}} \hat{B}_{i,j,t+1} + f_{y_{i,j,t+1}} \hat{y}_{i,j,t+1}] = 0,$$

which we rearrange to get the linear policy function,

$$m_{i,j,t} = a_m + b_m \tilde{\sigma}_{i,j,t}^2 + c_m \mathbb{E}_t \tilde{\sigma}_{i,j,t+1} + d_m \mathbb{E}_t B_{i,j,t+1} + e_m \mathbb{E}_t y_{i,j,t+1},$$

³⁵Due to the normality assumption for the liquidity shocks we can compute $\tilde{y}_{i,j} := \mathbb{E}(y_{i,j,t})$ analytically. Given $\tilde{y}_{i,j}$ we solve for the steady state values of $\tilde{m}_{i,j}, \tilde{\sigma}_{i,j}^2, \tilde{\lambda}_{i,j}$ under the absence of shocks to $\tilde{\sigma}_{i,j}^2$.

³⁶Computationally it is infeasible to compute $N(N-1)$ different expansion points depending on banks’ liquidity distribution.

that constitutes an approximate solution to the problem. Note that the intercept and the coefficients of the linear policy function are functions of the structural parameters.

APPENDIX B REDUCED FORM, STATIONARITY, AND ERGODICITY

Substituting the adaptive expectation mechanism in equations (11) and (12) into the Euler equation for monitoring in (8) and the optimal search strategy in equation (9) allows us to re-write the full system in reduced form. The reduced form can be written as a nonlinear Markov autoregressive process,

$$\mathbf{X}_t = \mathbf{G}_\theta(\mathbf{X}_{t-1}, \mathbf{e}_t),$$

where \mathbf{G}_θ is a parametric vector function that depends on the structural model parameter θ , and \mathbf{X}_t is the vector of all state-variables and control variables (observed or unobserved), and \mathbf{e}_t is the vector of shocks driving the system. These shocks are the liquidity shocks $\{\zeta_{i,j,t}^i\}$, the bank-to-bank-specific shocks to the perception-error variance $\{u_{i,j,t}\}$, and the shocks that determine if a link between any two banks is open and trade is possible $\{B_{i,j,t}\}$. Obtaining the reduced-form representation is crucial as it allows us to simulate network paths for both state and control variables under a given structural parameter vector. Furthermore, this model formulation allows us to describe conditions for the strict stationarity and ergodicity of the model that are essential for the estimation theory that is outlined in Section 4.

In particular, following Bougerol (1993), we find that under appropriate regularity conditions, the process $\{\mathbf{X}_t\}$ is strictly stationary and ergodic (SE).

LEMMA 1. *For every $\theta \in \Theta$, let $\{\mathbf{e}_t\}_{t \in \mathbb{Z}}$ be an SE sequence and assume there exists a (nonrandom) \mathbf{x} such that $\mathbb{E} \log^+ \|\mathbf{G}_\theta(\mathbf{x}, \mathbf{e}_t) - \mathbf{x}\| < \infty$ and suppose that the following contraction condition holds*

$$\mathbb{E} \ln \sup_{\mathbf{x}' \neq \mathbf{x}''} \frac{\|\mathbf{G}_\theta(\mathbf{x}', \mathbf{e}_t) - \mathbf{G}_\theta(\mathbf{x}'', \mathbf{e}_t)\|}{\|\mathbf{x}' - \mathbf{x}''\|} < 0. \quad (15)$$

Then the process $\{\mathbf{X}_t(\mathbf{x}_1)\}_{t \in \mathbb{N}}$, initialized at \mathbf{x}_1 and defined as

$$\mathbf{X}_1 = \mathbf{x}_1 \quad , \quad \mathbf{X}_t = \mathbf{G}_\theta(\mathbf{X}_{t-1}, \mathbf{e}_t) \quad \forall t \in \mathbb{N},$$

converges everywhere almost surely to a unique SE solution $\{\mathbf{X}_t\}_{t \in \mathbb{Z}}$ for every \mathbf{x}_1 , that is $\|\mathbf{X}_t(\mathbf{x}_1) - \mathbf{X}_t\| \xrightarrow{e.a.s.} 0$ as $t \rightarrow \infty$.³⁷

The condition that $\mathbb{E} \log^+ \|\mathbf{G}_\theta(\mathbf{x}, \mathbf{e}_t) - \mathbf{x}\| < \infty$ can be easily verified for any given distribution for the innovations \mathbf{e}_t and any given shape function \mathbf{G}_θ . The contraction condition in equation (15) is, however, much harder to verify analytically.

Fortunately, the contraction condition can be re-written as

$$\mathbb{E} \log \sup_{\mathbf{x}} \|\nabla \mathbf{G}_\theta(\mathbf{x}, \mathbf{e}_t)\| < 0 \quad (16)$$

where $\nabla \mathbf{G}_\theta$ denotes the Jacobian of \mathbf{G}_θ and $\|\cdot\|$ is a norm. By verifying numerically that this inequality holds at every step $\theta \in \Theta$ of the estimation algorithm, one can ensure that the simulation-based estimation procedure has the appropriate stochastic properties.

The contraction condition of Bougerol (1993) in equation (16) essentially states that the maximal Lyapunov exponent must be negative uniformly in \mathbf{x} .

DEFINITION 1. *The maximal Lyapunov exponent is given by $\lim_{t \rightarrow \infty} \frac{1}{t} \log \max_i \Lambda_{i,t} = \mathbb{E} \log \max_i \Lambda_{i,t}$ where $\Lambda_{i,t}$'s are eigenvalues of the Jacobian matrix $\nabla \mathbf{G}_\theta(\mathbf{x}_t, \mathbf{e}_t)$.*

A negative Lyapunov exponent ensures the stability of the network paths. Appendix Table 1 uses the Jacobian of the structural dynamic system $\mathbf{G}_\theta(\mathbf{x}, \mathbf{e}_t)$ to report numerical calculations of the maximal Lyapunov exponent of our dynamic stochastic network model at the parameters θ_0 and $\hat{\theta}_T$ described in Table 2 of Section 4.3. These points in the parameter space correspond to the starting point for the estimation procedure described in Section 4 and the final estimated point.

Appendix Table 1: Lyapunov Stability of the Dynamic Network Model

Parameter Vector	θ_0	$\hat{\theta}_T$
Lyapunov Exponent	-0.6451	-0.2462

Despite the higher degree of persistence at $\hat{\theta}_T$ compared to θ_0 (a higher Lyapunov exponent), the contraction condition is satisfied in both cases as the maximal Lyapunov exponent is negative.

³⁷A stochastic sequence $\{\xi_t\}$ is said to satisfy $\|\xi_t\| \xrightarrow{e.a.s.} 0$ if $\exists \gamma > 1$ such that $\gamma^t \|\xi_t\| \xrightarrow{a.s.} 0$.

This ensures that both θ_0 and $\hat{\theta}_T$ generate stable network paths.

APPENDIX C NETWORK AUXILIARY STATISTICS

In this section, we provide formulæ for the non-standard auxiliary statistics that characterize specifically the (dynamic) structure of the interbank lending network. First, the global network statistics that relate to the sparsity, reciprocity and stability are given as

$$\begin{aligned} density_t &= \frac{1}{N(N-1)} \sum_{i,j} l_{i,j,t}, & reciprocity_t &= \frac{\sum_{i,j} l_{i,j,t} l_{j,i,t}}{\sum_{i,j} l_{i,j,t}}, \\ stability_t &= \frac{\sum_{i,j} (l_{i,j,t} l_{i,j,t-1} + (1-l_{i,j,t})(1-l_{i,j,t-1}))}{N(N-1)}. \end{aligned}$$

Further, we maintain information about the *degree distribution*. In the interbank market, the degree centrality of a bank counts the number of different trading partners. For directed networks the out- and in-degree of node i are given by

$$d_{i,t}^{out} = \sum_j l_{i,j,t} \quad \text{and} \quad d_{i,t}^{in} = \sum_j l_{j,i,t}.$$

Instead of considering all $2N$ variables individually, we consider the mean, variance and skewness of the out-degree and in-degree distribution. The mean of degree distribution is proportional to the density. In the estimation procedure we include therefore only the average degree.

The (local) clustering coefficient of node i in a binary unweighted network is given by

$$c_{i,t} = \frac{1/2 \sum_j \sum_h (l_{i,j,t} + l_{j,i,t})(l_{i,h,t} + l_{h,i,t})(l_{j,h,t} + l_{h,j,t})}{d_{i,t}^{tot}(d_{i,t}^{tot} - 1) - 2d_{i,t}^{<->}},$$

where $d_{i,t}^{tot} = d_{i,t}^{in} + d_{i,t}^{out}$ is the total degree and $d_{i,t}^{<->} = \sum_{j \neq i} l_{i,j,t} l_{j,i,t}$ (see Fagiolo 2007). We consider the average clustering coefficient, defined as the mean of the local clustering coefficients.

Second, we compute simple bilateral local network statistics that measure the intensity of a bilateral trading relationship based on a rolling window of size $T_{rw} = 5$ (one five-day business week). As a simple measure of bilateral relationships, we compute the number of loans given from bank i to

bank j during periods $t' = \{t - T_{rw} + 1, \dots, t\}$ and denote this variable by

$$l_{i,j,t}^{rw} = \sum_{t'} l_{i,j,t'},$$

where the sum runs over $t' = \{t - T_{rw} + 1, \dots, t\}$. We then consider for each t the correlation between current access and past trading intensity, and between current interest spreads (for granted) loans and past trading intensity,

$$\text{Corr}(l_{i,j,t}, l_{i,j,t}^{rw}) \text{ and } \text{Corr}(r_{i,j,t}, l_{i,j,t}^{rw}).$$

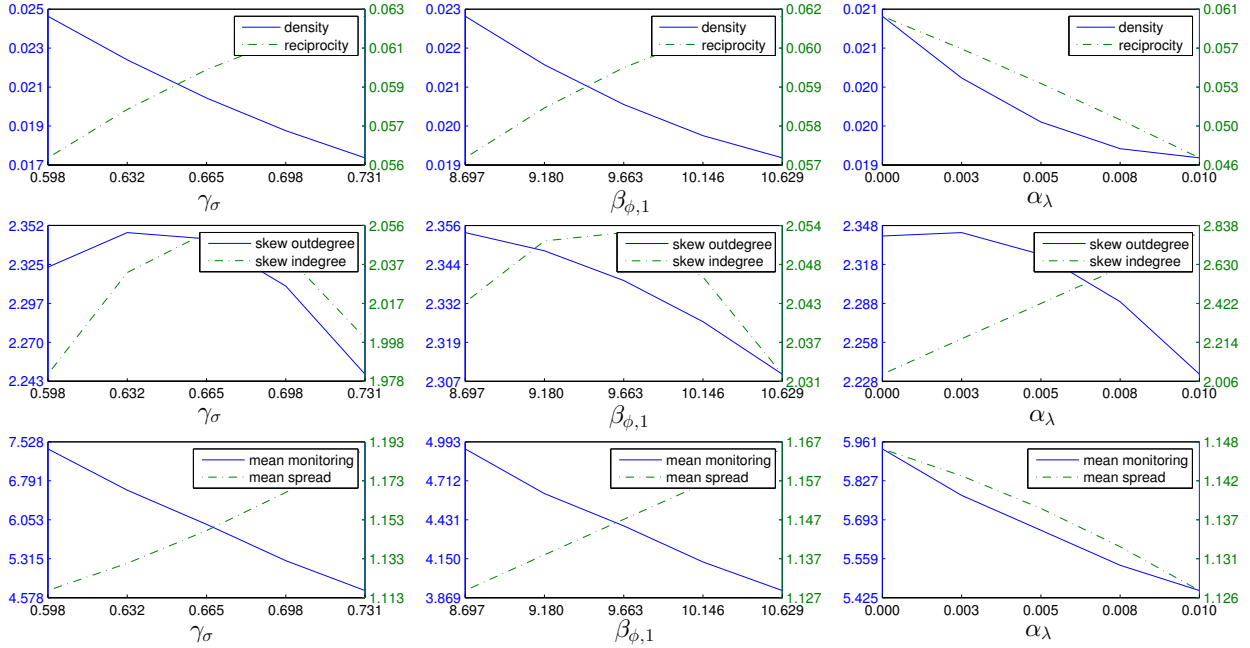
All described network statistics are computed for the network of interbank lending at each time period t such that we obtain a sequence of network statistics. We then obtain the unconditional means, variance and/or autocorrelation of these sequences as auxiliary statistics and base the parameter estimations on the values of the auxiliary statistics only.

APPENDIX D COMPARATIVE STATICS OF NETWORK STRUCTURES

In this section, we vary the structural parameters and analyze how the network structure responds as characterized by the auxiliary statistics. Appendix Figure 1 shows how the mean density, reciprocity, skewness of out-degree and in-degree distribution, mean monitoring and mean search respond to changes in structural parameters by ± 10 percent from their estimated values $\hat{\theta}_T$. Specifically, we focus on varying the coefficient of monitoring ($\beta_{\phi,1}$) in Equation (3), the autoregressive coefficient of the log perception-error variance (γ_σ) in Equation (1) and the parameter that determines the location of the logistic link probability function (α_λ), while holding constant all other parameters at the estimated values.

In the left panel, we see that an increase in the persistence of the log perception-error variance leads to a lower network density and a higher fraction of reciprocal lending relationships. Moreover, for the plotted range of values of γ_σ , both the in- and out-degree skewness exhibit a hump shaped form. For a low persistence in credit-risk uncertainty, an initial increase in γ_σ leads to higher skewness of the degree distributions, in particular the in-degree becomes more asymmetrically distributed. Economically, as the persistence of credit-risk uncertainty increases, some banks lose

Appendix Figure 1: Comparative Statics of Network Statistics



Notes: Simulated mean of network statistics as a function of key structural parameters related to credit-risk uncertainty (γ_σ), efficacy of peer monitoring ($\beta_{\phi,1}$), and search frictions (α_λ). Parameters range from ± 10 percent around estimated values, holding fixed all other parameters. Each figure is based on 5,000 MC repetitions, each with $T = 500$. Left (right) axes correspond to solid (dashed) lines. Source: Authors' calculations.

trading partners—which potentially cuts off their access to the interbank market—while few highly connected banks can still maintain sufficiently many lending relations (these money center banks are intensively monitored, as they are frequent large-volume borrowers). As the uncertainty increases further, however, lender banks will also occasionally refrain from providing credit to money center banks, and the skewness decreases again. In addition, more persistent uncertainty leads to higher spreads of granted loans and decreases monitoring efforts due to lower profitability.

The network shows a qualitatively similar response to a local increase in the marginal effect of monitoring on the added information; specifically, the density decreases and lending becomes more reciprocal (center panel). At the same time, the average spread of granted loans increases and banks on average reduce peer monitoring efforts (bottom plot). The decline in monitoring occurs because $\frac{\partial \pi_{i,t}}{\partial m_{i,j,t} \partial \beta_{\phi,1}} \Big|_{\theta=\hat{\theta}} < 0$ for sufficiently large $m_{i,j,t}$, in particular at the expansion point of the first order conditions. Intuitively, banks' steady-state monitoring levels are such that uncertainty is already relatively low, and an increase in $\beta_{\phi,1}$ further reduces the marginal benefits from monitoring. To

maintain the equality between the (constant) marginal cost and benefit, it is necessary to reduce monitoring efforts. The results confirm our findings where we compare the results for the estimated model with those for a model without monitoring ($\beta_{\phi,1} = 0$).

The right panel reveals that if banks need to invest more to maintain the same link probability, less trading occurs and lending becomes less reciprocal because some banks will not find it profitable to maintain some of their trading relationships. However, as the large increase in the in-degree skewness suggests, at the borrower level, the reduction in lending partners is again asymmetrically distributed. In particular, as the cost of link formation increases, borrowing becomes more concentrated toward few highly connected core banks. At the same time, the reduction in out-degree skewness reflects that highly connected lenders lose some of their borrowers that don't find it profitable anymore to incur the search cost, thereby reducing the asymmetry of the degree distribution. Moreover, while the average monitoring expenditures decrease as a reaction to the higher cost of linking, the mean spread of granted loans decreases because those bank pairs that continue trading have lower uncertainty about their counterparts.

APPENDIX E SUMMARY STATISTICS

Appendix Table 2: Descriptive Statistics of Dutch Interbank Network

Statistic	Mean	Std	Autocorr	Skew	Kurtosis
Density	0.0212	0.0068	0.8174	0.8667	3.1983
Reciprocity	0.0819	0.0495	0.2573	0.2903	2.8022
Stability	0.9818	0.0065	0.8309	-0.8590	3.0503
Mean Out-/In-degree	1.0380	0.3323	0.8174	0.8667	3.1983
Std Out-degree	1.8406	0.4418	0.6882	0.0553	2.4326
Skew Out-degree	2.8821	1.0346	0.7035	0.6074	2.4572
Mean In-degree	1.0380	0.3323	0.8174	0.8667	3.1983
Std In-degree	1.6001	0.4140	0.6880	0.6997	3.4529
Skew In-degree	2.4030	0.8787	0.6576	0.6714	2.7434
Mean Clustering	0.0308	0.0225	0.4149	0.7900	3.2473
Std Clustering	0.0880	0.0490	0.3587	0.1561	2.7280
Skew Clustering	3.7367	1.5454	0.1213	-0.2213	3.1281
Avg Log Volume	4.1173	0.2818	0.4926	-0.2820	2.8220
Std Log Volume	1.6896	0.1685	0.3623	0.1541	3.4546
Skew Log Volume	-0.3563	0.2818	0.2970	-0.0669	3.2151
Avg Spread	0.2860	0.3741	0.9655	1.1044	2.6965
Std Spread	0.1066	0.0632	0.7865	1.6668	6.8848
Skew Spread	0.6978	1.6399	0.5492	0.6832	2.9469
Corr($r_{i,j,t}, l_{i,j,t}^{rw}$)	-0.0716	0.1573	0.4066	0.0817	2.8539
Corr($l_{i,j,t}, l_{i,j,t}^{rw}$)	0.6439	0.0755	0.4287	-0.7653	4.2833

Notes: The table shows moment statistics for different sequences of network statistics and cross-sectional correlations that characterize the sequence of observed Dutch unsecured interbank lending networks. The statistics are computed on a sample of daily frequency from February 18, 2008, to April 28, 2011.